Azoheteroarene Based Ligands for Metal Binding and Solid State Photochromism

Vaitheesh Jeyapalan

MS14007

A dissertation submitted for the partial fulfilment of BS-MS dual degree in Science

INDIAN INSTITUTE OF SCIENCE EDUCATION AND RESEARCH MOHALI

APRIL 2019

Certificate of Examination

This is to certify that the dissertation titled "Azoheteroarene Based Ligands for Metal Binding and Solid State Photochromism" submitted by Mr. Vaitheesh Jeyapalan (Reg. No. MS14007) for the partial fulfilment of BS-MS dual degree programme of the Institute, has been examined by the thesis committee duly appointed by the Institute. The committee finds the work done by the candidate satisfactory and recommends that the report be accepted.

Dr. Santanu Kumar Pal	Dr. Sripada S.V. Rama Sastry	Dr. Sugumar Venkataramani
(Committee Member)	(Committee Member)	(Supervisor)

Dated: April , 2019

Declaration

The work presented in this dissertation has been carried out by me under the guidance of Dr. Sugumar Venkataramani at Indian Institute of Science Education and Research Mohali.

This work has not been submitted in part or in full for a degree, a diploma, or a fellowship to any other university or institute. Whenever contributions of others are involved, every effort is made to indicate this clearly, with due acknowledgement of collaborative research and discussions. This thesis is a bonafide record of original work done by me and all sources listed within have been detailed in the references.

Vaitheesh Jeyapalan
(Candidate)
Dated: April , 2019

In my capacity as the supervisor of the candidate's project work, I certify that the above statements by the candidate are true to the best of my knowledge

Dr. Sugumar Venkataramani
(Supervisor)

Dedicated to

(Ankit, Debo, Anjali and friends)

Acknowledgement

I am thankful to: Dr. Sugumar Venkataramani for the training and guidance, that he provided throughout the course; Dr. N. Sathyamuthy [ex-Director, IISER Mohali], Dr. Arvind [Director, IISER Mohali], Dr. K. S. Viswanathan [ex-Head of Department of Chemical Sciences, IISER Mohali] and Dr. S. Arulananda Babu [Head of Department of Chemical Sciences, IISER Mohali], for providing me with the opportunity and facilities required to successfully complete my coursework; Dr. Santanu Kumar Pal and Dr. Sripada S.V. Rama Sastry for agreeing to be in my thesis committee and their valuable inputs throughout the coursework; Dr. Sanjay Singh, Sandeep Thakur and his lab members for helping me with crystallisation and retrieval of single crystal XRD data; Dr. Angshuman Roy Choudhury, Mayank Joshi and lab members for helping with PXRD studies.

I would also like to register my sincere gratitude towards Ankit, Debapriya, and Himanshu for their selfless efforts, guidance, care and love they had showered upon me. I am especially indebted to Anjali, Ankit and Debo for being there for me when I was in doubt and helping me find my motivation. I would like to thank all the members of the Physical Organic Chemistry lab, IISER Mohali for providing me with a safe and enjoyable work environment.

Finally, I would like to thank the “silent guardians and watchful protectors”- Abin, Balu and Jain for befriending me, sharing their lives with me, for witnessing me at my worst and being there for me whenever I needed them for the past demi-decade; Joji, Ganga, Awani and Adheena for all the time spent together, being the lifelines that I needed; Sachiku, Swetha and nunu for late night binging sessions, food dates and for being absolute darlings.

List of Figures

List of Tables

Notations

UV- Ultraviolet

NMR- Nuclear Magnetic Resonance

HRMS- High Resolution Mass Spectrometry

XRD- x-Ray Diffraction

EtOAc- Ethyl Aceate

HCl- Hydrochloric acid

H_2O- Water

EtOH- Ethanol

MeOH/CH_3OH- Methanol

N_2H_4- Hydrazine

$SOCl_2$- Thionyl Chloride

$CHCl_3$- Chloroform

DCM- Dichloro Methane

NaH- Sodium Hydride

DMF- Dimethyl Formamide

K_2CO_3- Potassium Carbonate

CH_3CN- Acetonitrile

NaN_3- Sodium Azide

$CuSO_4.5H_2O$- Copper Sulfate Pentahydrate

$NiCl_2.6H_2O$- Nickel Chloride Hexahydrate

$CoCl_2.6H_2O$- Cobalt Chloride Hexahydrate

$CuCl_2.2H_2O$- Copper Chloride Dihydrate

NH_4PF_6- Ammonium Hexafluoro Phosphate

KBr- Potassium Bromide

$CDCl_3$- Deuterated Chloroform

DMSO- Dimethylsulfoxide

KCl- Potassium Chloride

Contents

Abstract

Photoswitchable molecules can be switched optically between two or more stable forms that can exhibit different physical properties. Due to their ability to translate incoming non-invasive, monochromatic light stimulus to trigger macroscopic property changes, they show great prospect in molecular electronic and photonic devices, biological and medicinal applications, and other material chemistry applications. Incorporation of organic photochromic units in known transition metal complexes can provide control over the physiochemical properties of the complexes. Among the photo active building blocks available, azoheteroarenes especially arylazopyrazoles show efficient and reversible photo-isomerization (E-Z) in both solid and solution phases. Moreover, high half-life has been reported for the thermodynamically unstable cis-isomer of arylazopyrazoles. The visible changes in colour between the cis- and trans-isomers of arylazopyrazoles even in the solid state has led to their application in rewritable imaging techniques. Since pyrazole based chelating ligands have been known to form a variety of coordination complexes with a number of transition metals, we have attempted to incorporate photo-active arylazopyrazole units in some of the known chelating ligands and study the systematic tuning of the colour and photoswitching properties of the resulting photo-active complexes.

Chapter 1: Introduction

1.1. Photoswitches

Photoswitches are molecules, which reversibly transform light energy by undergoing phototransformations between two or more stable forms with different physical properties (geometry, rigidity, absorption spectra, dielectric constant and refractive index)[1]. Due to their ability to translate incoming non-invasive, monochromatic light stimulus into changes in geometry, molecular photoswitches can induce changes in structure at molecular length scale when incorporated within liquid crystal or polymer frameworks[2]. This is why in the recent years, there has been an unprecedented surge in application of photoswitches in molecular electronic and photonic devices, biological and medicinal applications, and other material chemistry applications[3]. To address the limitations of presently available chemically or photoinduced switches, researchers are trying to come up with new molecular switch architectures, which are specifically suited for certain applications[4].

The performance of a photoswitch is evaluated based on four main parameters-

a) Thermal stability of both photoisomers- Applications such as optical data storage or photopharmacology requires both the photoisomers to have considerable half-lives under ambient temperature conditions.

b) Photostationary state (PSS)- This is expressed as the ratio of relative abundance of one photoisomer over the other after exposure to a certain wavelength light.

c) Reversibility- The photoswitch should not exhibit signs of fatigue even after several cycles of switching.

d) Last but not the least, the wavelength for photoisomerization. For biological applications, the photoswitches should switch within the bio-optical window.

Although a number of organic photoswitches like spiropyrans, oxazines, stilbenes, indigoids etc. are well known, the oldest known photoswitches, azobenzene is still preferred in a large number of applications, because of ease of synthesis, ease of functionalization, large extinction coefficients, reasonable quantum yields, reversibility in switching and high percentage of *E*-*Z* isomerization.

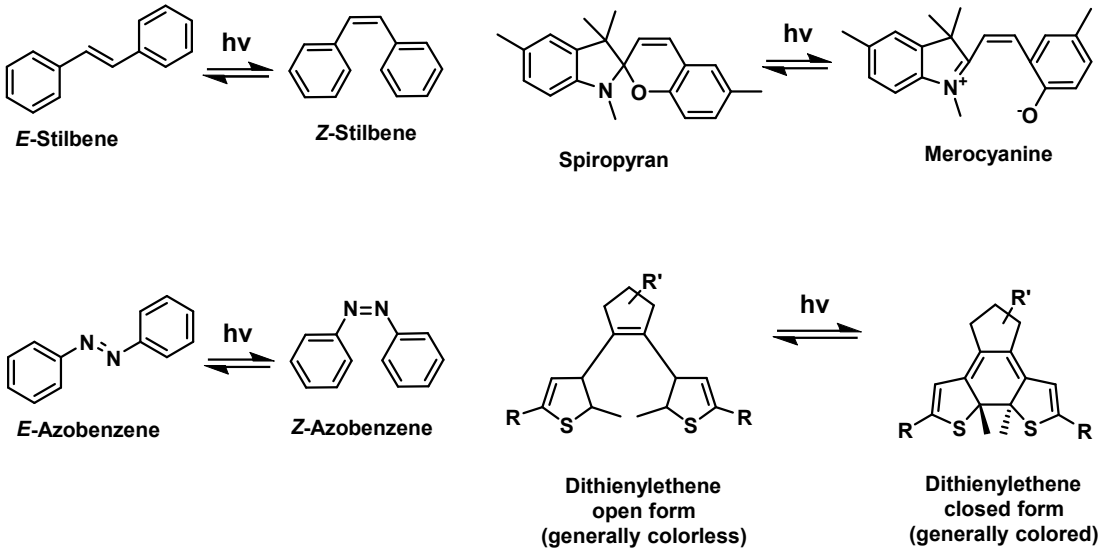

Scheme 1.1. Structures of different photoswitches.

1.2. Azobenzenes and isomerization mechanism

Azobenzenes can exist in both *E*- and *Z*-isomeric forms. The *E*-isomer adopts a planar structure with C_{2h} symmetry, while the *cis*-isomer adopts a non-planar configuration. The *E*-isomer has a distinct UV spectrum consisting of a weakly allowed n-π* transition from ground state S_0 to singlet excited state S_1 in a visible range and symmetry allowed intense π-π* transition from S_0 to second excited state S_2[5]. Exposure to UV light irradiation converts the thermodynamically stable *E*-isomer to *Z*-isomer. Photoisomerization changes a number of physical properties including a marked difference in absorption spectra (intensification of n-π* band and prominent blue shift in π-π* band). Isomerization can happen from either S_1 or S_2 through a conical intersection that connects S_1 and S_0 states. A torsional pathway assisted by inversion has been proposed for the photoisomerization of azobenzenes, involving in-plane motion and out-of-plane rotation. The *Z*-*E* photoisomerization can be done both photochemically and/or thermally. A number of mechanisms including rotation and/or inversion mechanisms have been proposed for the thermal reverse isomerization step.

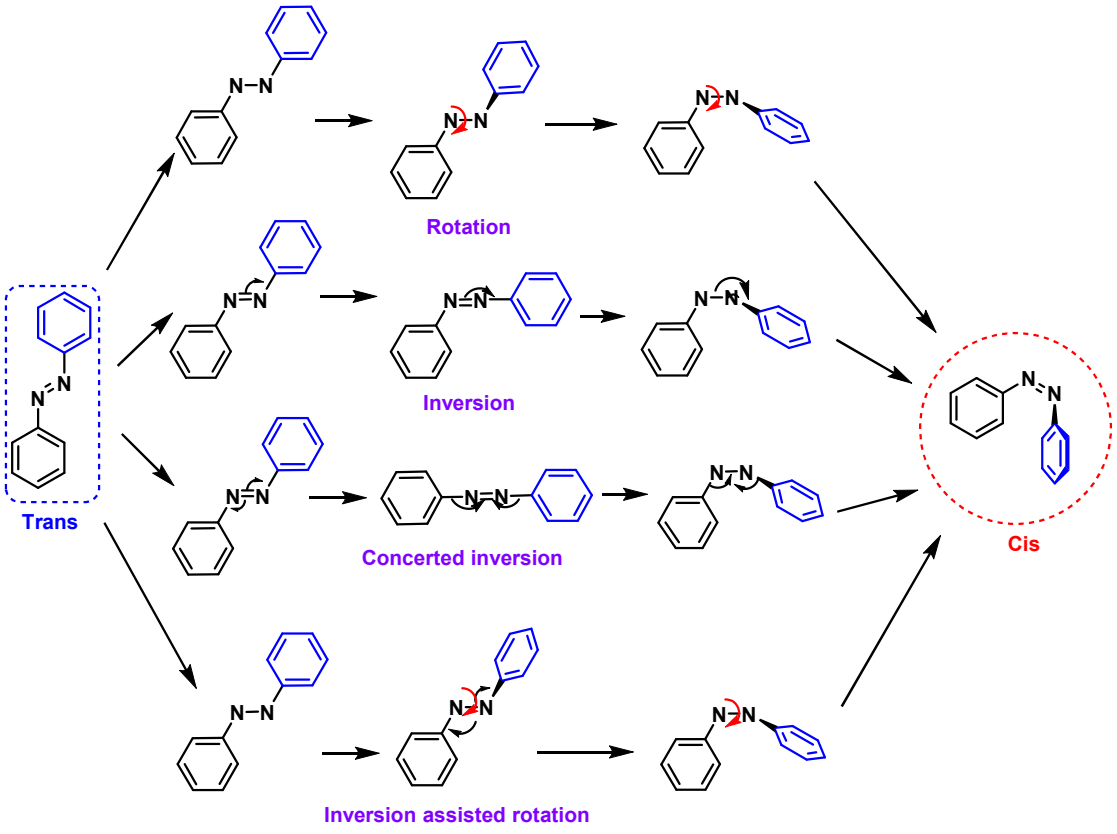

Scheme 1.2. Mechanisms of *E*- & *Z*-isomerisation in Azobezene

1.3. Structurally modified azobenzenes and azoheteroarenes

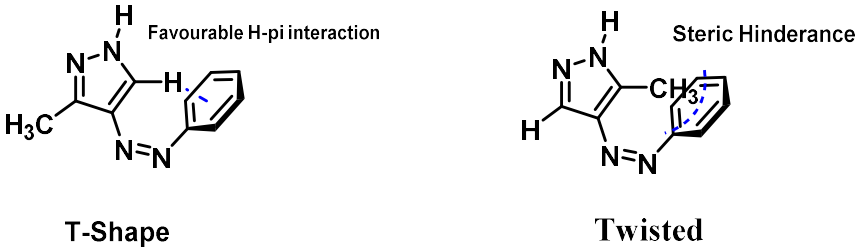

Scheme 1.3. Structures of azoheteroarenes t-shaped & twisted geometry in *cis*-isomeric form

In the last decade, investigations on azobenzene has primarily been focused on introducing structural modification to ensure: a) photoswitching with visible light (The

quest of getting azobenzene to switch with visible light has produced numerous examples of red-shifted absorption maxima by introducing multiple substitution to position *ortho*- to the azo group like methoxy or fluorine atoms[6]); b) creating a photoswitchable system capable of high percentage of *E*-*Z* conversion along with long half-life of *Z*-isomer and excellent reversibility (Along with some structurally modified azobenzenes, some of the azoheteroarenes, where the heterocyclic ring is a five membered ring are known to show excellent percentage of conversion to *Z*-isomer and long thermal half-lives of *Z*-isomer[7]). *Z*-isomer of a five membered azoheteroarene can access either a twisted or a T-shaped geometry, either of which is inaccessible to normal azobenzenes. The preference of one geometry over another is decided by the number of substituents in the *ortho*-position with respect to azo group. While introducing one methyl substitution may result in T-shaped geometry (with outward orientation of methyl group) over the twisted structure (with inward orientation of methyl group). The azoheteroarene with methyl substitution in both *o*-positions can only adapt a twisted geometry in the *Z*-isomer. Apart from the geometry of *Z*-isomer, the frontier molecular orbitals of various azoheteroarenes have been thoroughly investigated. A number of other factors including steric, electronic and hydrogen bonding and solvent effects influence the stability of *Z*-isomer[7-8]. Since being introduced as quantitative photoswitches with excellent reversibility and long half-life in 2016[9], arylazopyarazoles have been used in a number of applications including photopharmacology and solid state switchable materials for imaging/erasing applications[10]. However in only one instance, arylazopyrazoles have been used as part of an organic photochrome introduced in the ligand framework of a coordination complex leading to a photoswitchable metal complex[11]. Incorporation of organic photochromic units in ligand frameworks of coordination complexes results in photoswitchable coordination complexes[12]. Such complexes have found their applications primarily in non-linear optics, spin crossover research and photoswitchable catalysis[13]. However, in most of these cases, the photoswitchable unit used is based on azopyridines and azoimidazoles. Since numerous examples of pyrazole based ligands are available in transition metal chemistry and these ligands can coordinate with different metals to produce complexes of different geometry [14], arylazopyrazole based photoswitchable ligands can lead to new directions in coordination and supramolecular chemistry.

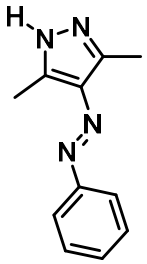

Arylazopyrazole

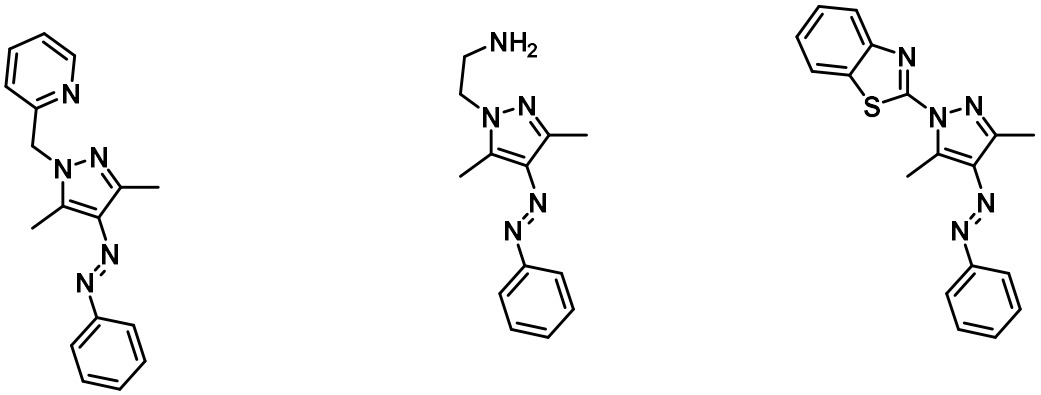

Photoswitchable arylazopyrazole based ligands

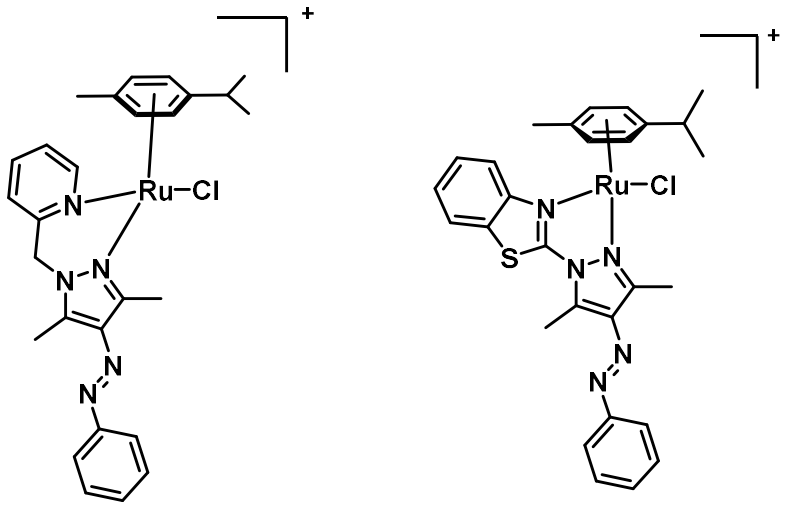

Photoswitchsale arylazopyrazole- containing Ruthenium (II) p-cymene complexes

Scheme 1.4. Arylazopyrazole; examples of arylazopyrazole based ligands and arylazopyrazole ruthenium complexes [adapted from *Organometallics*, **2017**, *36*,3360]

1.4. Transition metal coordination effects on photochromic ligands

The development of transition metal coordination complexes with photo-active ligands incorporated with photochromic moieties has received attention in the past decade[15]. By designing photochromic moieties as ligands, the photoswitching properties can be systematically tuned and differed by relatively simple coordination to different metal centres. Development of photochromic ligands for coordination to metal complex systems represents an alternative approach to adjust the photochromic properties without the need to vary the organic framework through tedious synthetic approaches. The change in electronic structure associated with photochromic reactivity could on the other hand, switch the properties of the metal complexes[12].

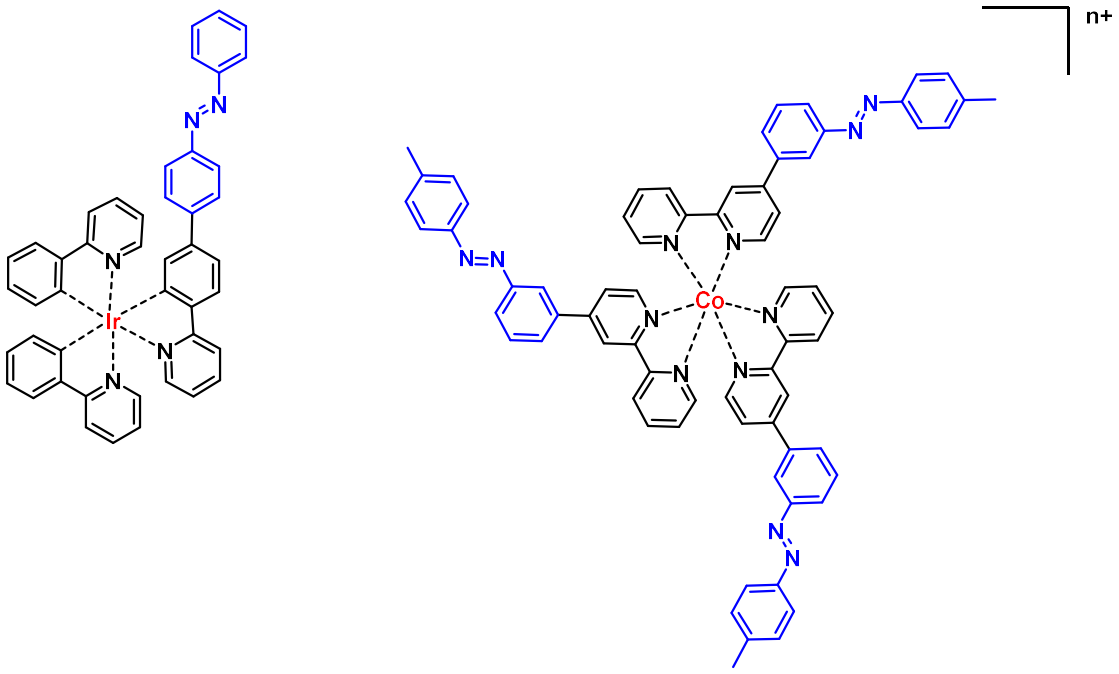

Scheme 1.5. Azobenzene transition metal complexes.

1.5. Aim of the project

The aim of this project was to incorporate the photoswitchable arylazopyrazole motif within some of the well-known pyrazole based ligand framework and study photoswitching of these complexes. We approached the project in four steps: 1.

Identifying pyrazole based ligands where arylazopyrazoles can be incorporated within the ligand framework easily; 2. Incorporation of arylazopyrazole as the photoswitchable unit within the ligand framework and systematically studying the photoisomerization of the ligand by UV-vis and NMR spectroscopy; 3. Complexation of the ligand with different transition metals and determination of the structure of the complexes by XRD. 4. Studying the photoswitching of the complexes by UV-vis and NMR spectroscopy and extensive comparison of the photophysical properties of the complex with that of the ligand.

Pyrazole based scorpionate ligands are well known in transition metal chemistry. Although a number of ligand frameworks of different geometry are available, we have chosen one particular ligand framework because of: A. Ease of synthesis: arylazopyrazole as a photoswitchable unit can be easily incorporated within the ligand framework by a simple substitution reaction; B. Pincer Ligands: The NNN pincer framework with pyrazole as a chelating unit allows complexation of the ligand to a number of transition metals while allowing us the possibility of having multiple photoswitchable units within the same ligand framework.

We have chosen 3,5-disubstituted arylazopyrazole as the photoswitchable unit based on four main factors: (a) High percentage of *E*-*Z* conversion which can be quantified by NMR spectroscopy; (b) Long half-life of *Z*-isomer, which allows enough time for studying the photophysical properties of the thermodynamically unstable photoisomer; (c) Excellent reversibility: system shows zero fatigue even after several photoswitching cycles; (d) Solid state photoswitching- 3,5-substituted arylazopyrazole derivatives are well known solid state switches with marked difference in the colour of *E*- and *Z*-isomer. We hypothesized that the incorporation of this photoswitchable unit within the ligand framework will lead to solid state photoswitching of the coordination complex resulting in a change of physical properties including the colour of the complexes.

Chapter 2: Results and discussion

2.1. Design rationale

The goal of our project was to synthesize photoswitchable chelating ligands that show reversible photoswitching and photochromic behaviour in both liquid and solid states as well as metal binding and coordinating prospects. The target ligands **L1-L3** are bipodal and tripodal pincer type N donor ligands. **L1** has two pyrazole units as N-donor units, while for **L2** and **L3**, there is an additional N-donor centre. (For **L2**, it is a pyridine, whereas a triazole unit has been used in **L3).**

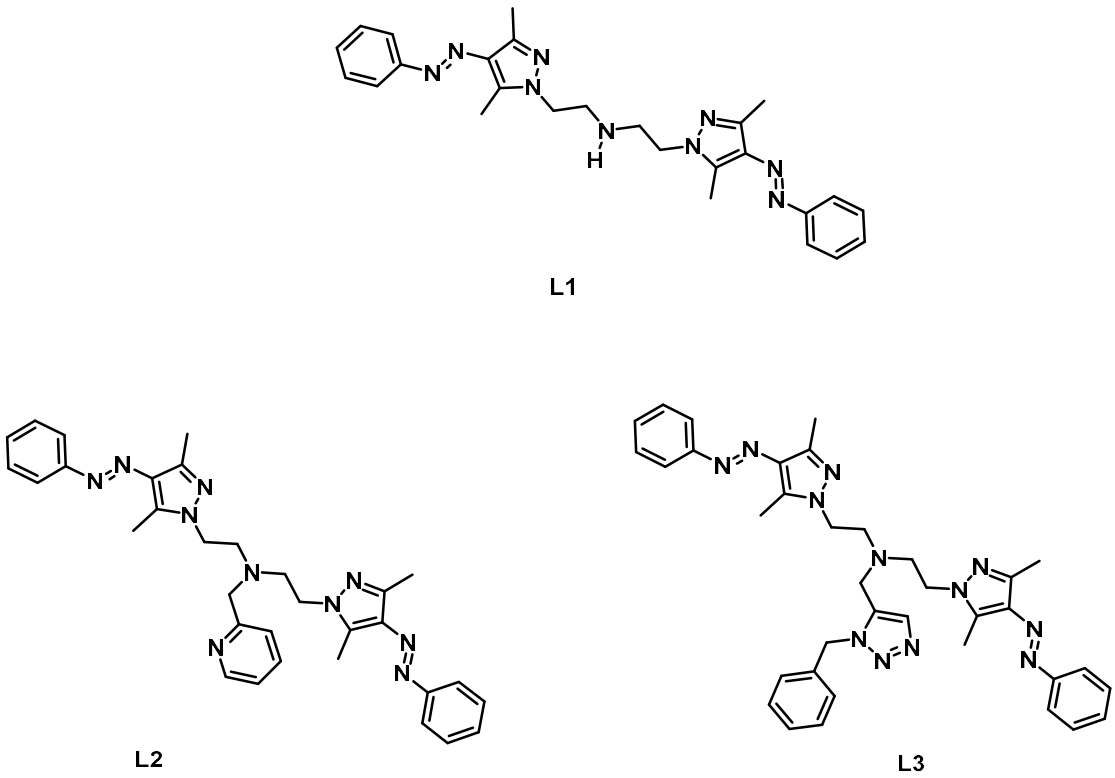

Scheme 2.1 Target ligand **L1**, **L2** and **L3**

2.2. Synthesis of photoswitchable unit [P1]

The first step in our project was to synthesise the photoswitchable unit **P1** to be incorporated into our target molecules. For the synthesis of **P1**, the reaction scheme has been adopted from literature[8a]. First, 3-(2-phenyldiazenyl)-2,4-pentanedione was prepared by diazotization of aniline, and consequent reaction of diazonium salt with

acetylacetone. Precipitate was collected, washed with water and isolated using column chromatography (1:19 EtOAc:Hexane). In the next step, (E)-3-(phenyldiazenyl)pentane-2,4-dione was reacted with hydrazine monohydrate in ethanol to prepare **P1**. After evaporation of ethanol, reaction mixture was extracted using ethyl acetate and washed with water and brine. Product was purified by silica-gel column chromatography with 1:1 ethyl acetate:hexane as eluent. Product was confirmed by NMR and HRMS with 89 % yield.

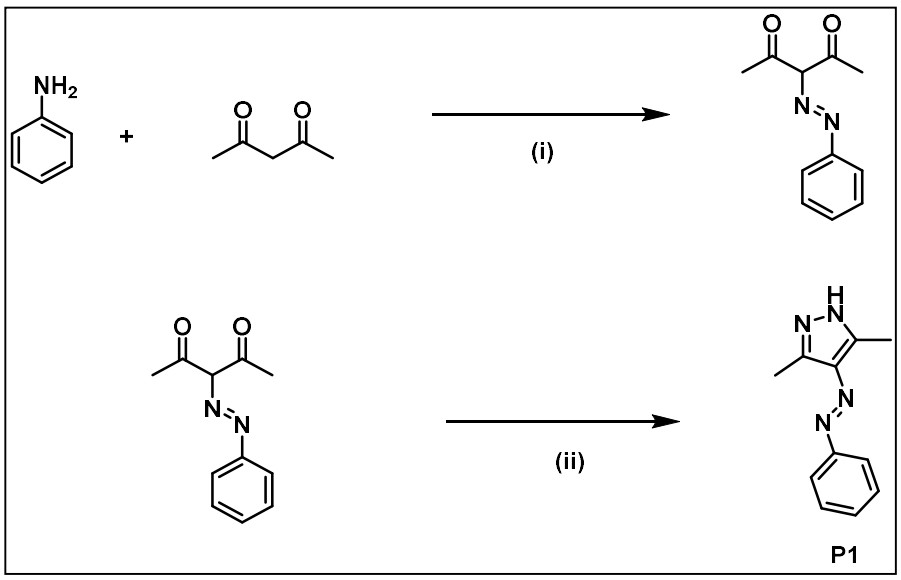

Scheme 2.2. Synthetic scheme **P1.** (i) $NaNO_2$, Sodium acetate, HCl, H_2O/EtOH (1:1), 0 ºC, 3h, 82%; (ii) $N_2H_4.H_2O$, EtOH, reflux, 3h, 89%

2.3. Synthesis of P1 incorporated photo-active chelating ligands.

The next step in our project is to incorporate the synthesised photoswitchable system [**P1**] within the ligand frameworks and synthesise target photo-active, chelating ligands. (**L1**-**L3**)

2.3.1 Synthesis of photoswitchable ligand L1

For the synthesis of our target ligand **L1**, we first synthesised bis(2-Chloroethyl) amine hydrochloride. For its synthesis, we have adapted a procedure reported in the literature[15] (Ref. Scheme 2.3). The product was filtered off, washed with chloroform, diethyl ether and dried under vacuum. (Yield = 78%)

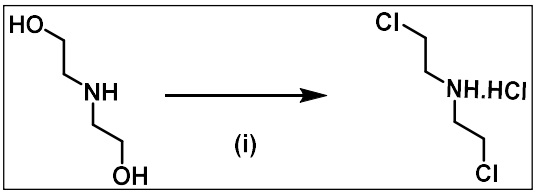

Scheme 2.3. Synthetic Scheme of bis(2-chloroethyl) amine hydrochloride. (i) $SOCl_2$, $CHCl_3$, reflux, 1h, 78%

Using bis(2-Chloroethyl) Amine hydrochloride, the synthesis of our target ligand **L1** was carried out, and the reaction conditions were adopted from a known reported procedure[16] (Ref. Scheme 2.4). The solid precipitate was filtered off, and the product was extracted using DCM, and washed with water and brine. Volatiles were removed under reduced pressure. The product was purified by silica gel column chromatography with ethyl acetate as an eluent. The product was confirmed by NMR and HRMS with 82% yield.

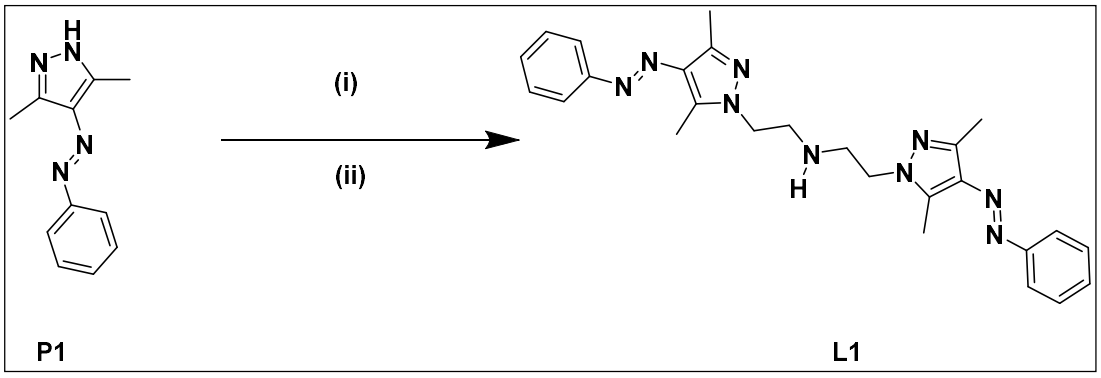

Scheme 2.4. Synthetic scheme of **L1.** (i) NaH, DMF (dry), rt, 2h; (ii) bis(2-Chloroethyl) Amine hydrochloride, DMF (dry), 70 °C, 2h, 82%

2.3.2. Synthesis of photoswitchable ligand L2

Synthesis scheme of target photoswitchable ligand [**L2**] has been adapted from literature[16] (Ref. Scheme 2.5). Once again precipitates were filtered off, extracted using ethyl acetate, washed with water and volatiles were removed under reduced pressure. Product was purified by silica-gel column chromatography with ethyl acetate as an eluent. The product was confirmed by NMR and HRMS with 80% yield.

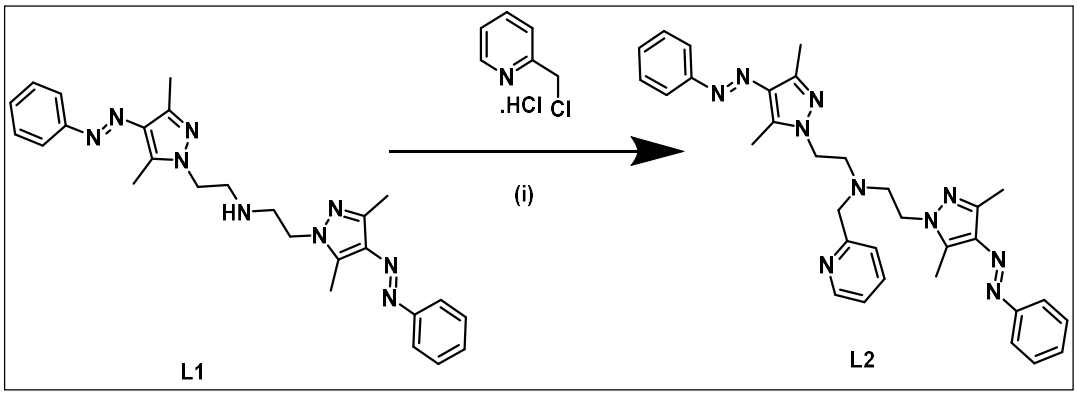

Scheme 2.5. Synthetic scheme of **L2.** (i) K_2CO_3, CH_3CN, N_2 atmosphere, reflux, 3d, 80%

2.3.3. Synthesis of photoswitchable ligand L3

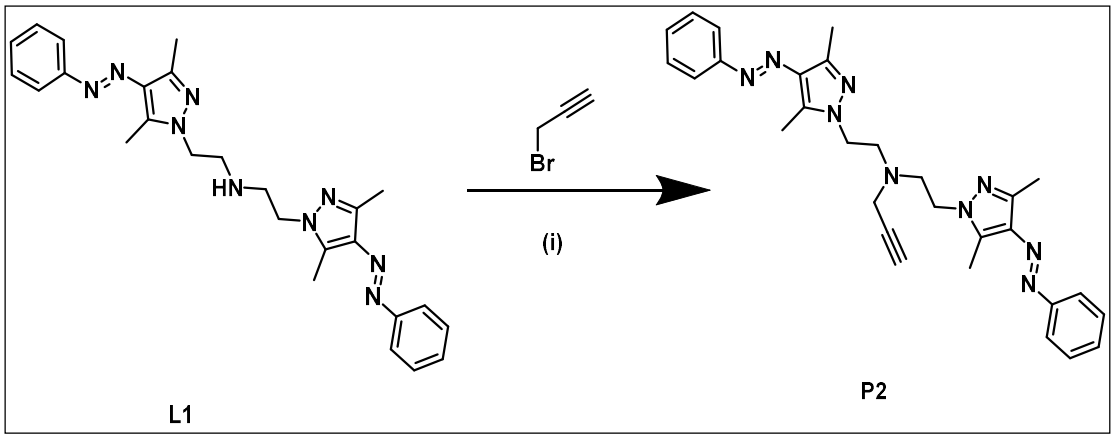

Scheme 2.6. Synthetic scheme of **P2.** (i) K_2CO_3, CH_3CN, rt, overnight, 67%

As a preliminary step towards the synthesis of our target ligand, the alkyne precursor [**P2]** has been synthesised by following the synthesis scheme given in Scheme 2.6. The synthesis strategy has been adopted from literature [17]. K_2CO_3 was filtered off from the dark brown suspension containing the product. The product was extracted using ethyl acetate and washed with water and brine. Purification of product was attempted using column chromatography in basic alumina with ethyl acetate as eluent. Unfortunately, even after several attempts, the product could not be purified. The product was confirmed by HRMS.

The precursor thus synthesised was then subjected to a reaction (without isolation) according to the synthetic scheme given in Scheme 2.7. The synthesis strategy has been adopted from literature[17]. Precipitates were filtered off from the reaction mixture. Product was extracted with chloroform and washed with water and brine. The product could not further be isolated using column chromatography. However, the product was confirmed by HRMS.

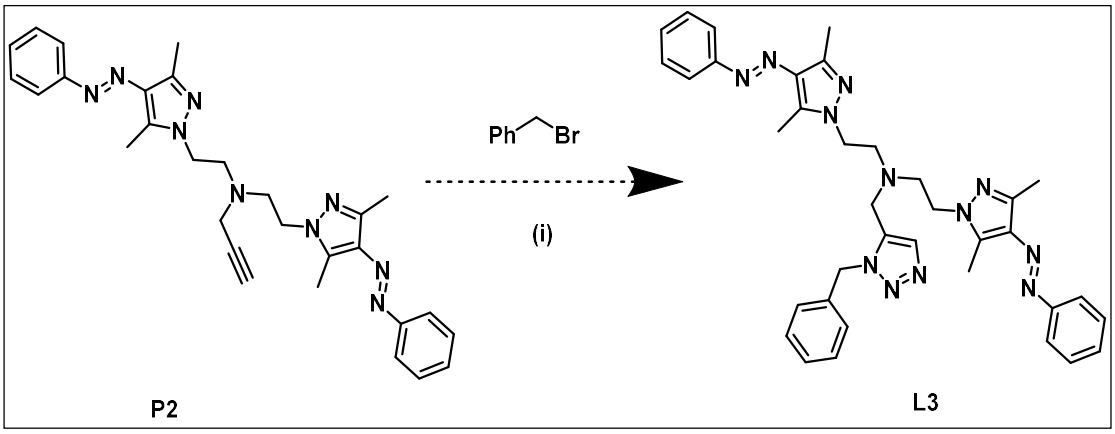

Scheme 2.7. Synthetic scheme of **L3.** (i) NaN_3, Sodium ascorbate, $CuSO_4.5H_2O$, DMF/H_2O (4:1), 82 ^oC, overnight.

2.4. Metal complexation

We have attempted to synthesise transition metal coordination complexes with the arylazopyrazole incorporated photo-active ligands, and study the systematic tuning of colour and the photoswitching properties of these photo-active complexes. Initially, we tried mixing solutions of different transition metals with the solution of the synthesised ligands. In some of the cases, the resultant solutions were of different colours and exhibited photochromic behaviour upon excitation by light stimulus. From these solutions, a few were selected on the basis of the visible changes in colour that they produced after irradiation with UV light. These selected metal salts were used to synthesise metal coordination complexes with the photo-active ligands.

2.4.1. Synthesis of metal coordination complexes with photo-active ligand L1

Based on the metal binding and screening experiment, $NiCl_2.6H_2O$, $CoCl_2.6H_2O$ and $CuCl_2.2H_2O$ salts were selected to form the coordination complex with ligand **L1**. The synthesis of the metal coordination complex was undertaken according to the schemes provided in Scheme 2.8-2.10. These synthesis schemes were adapted from similar schemes reported in literature[18]. The product was extracted by removing the solvents under reduced pressure. The product was confirmed by HRMS with around 70% yield and kept for crystallization in ACN, MeOH and 1:1 ACN: MeOH.

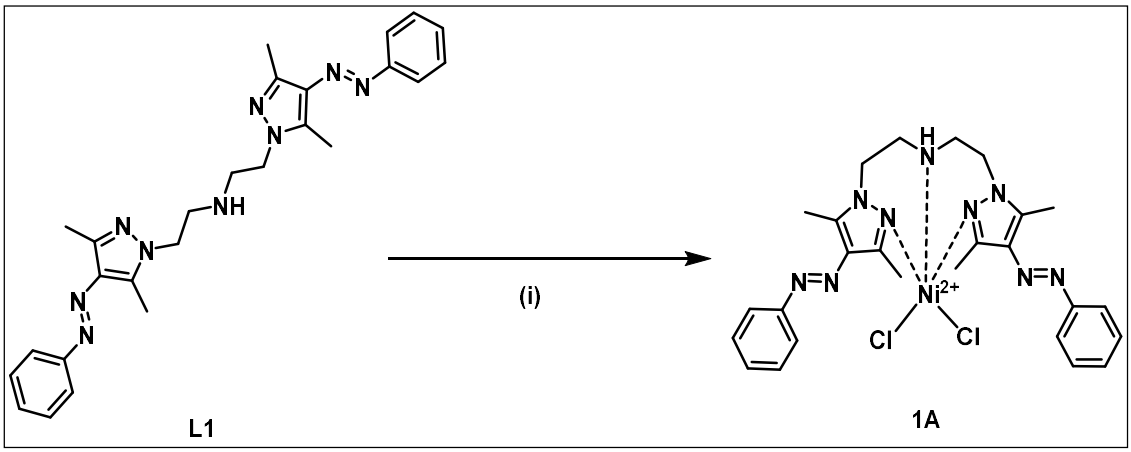

Scheme 2.8. Synthetic Scheme of Metal coordination complex **1A.** (i) $NiCl_2.6H_2O$, CH_3OH, rt, overnight, 76%.

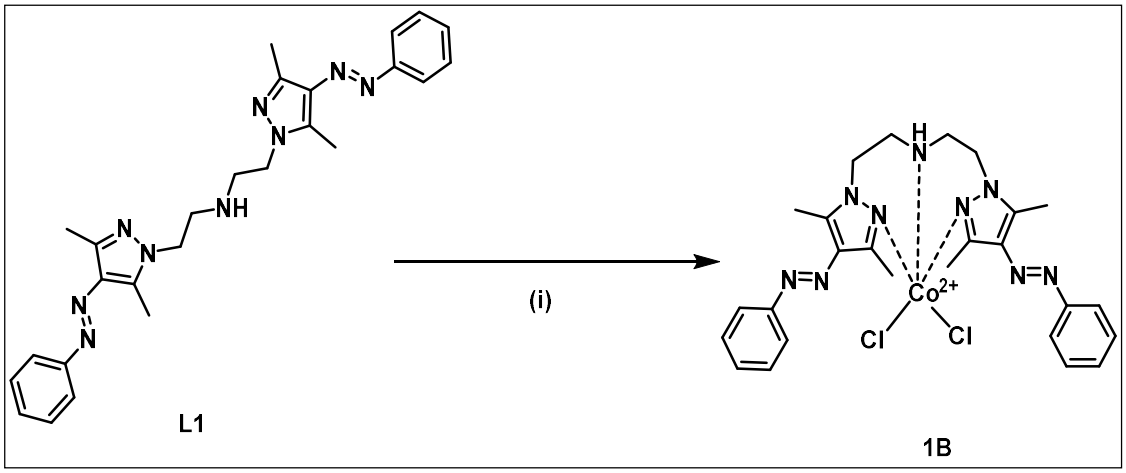

Scheme 2.9. Synthetic Scheme of Metal coordination complex **1B.** (i) $CoCl_2.6H_2O$, CH_3OH, rt, overnight, 72%.

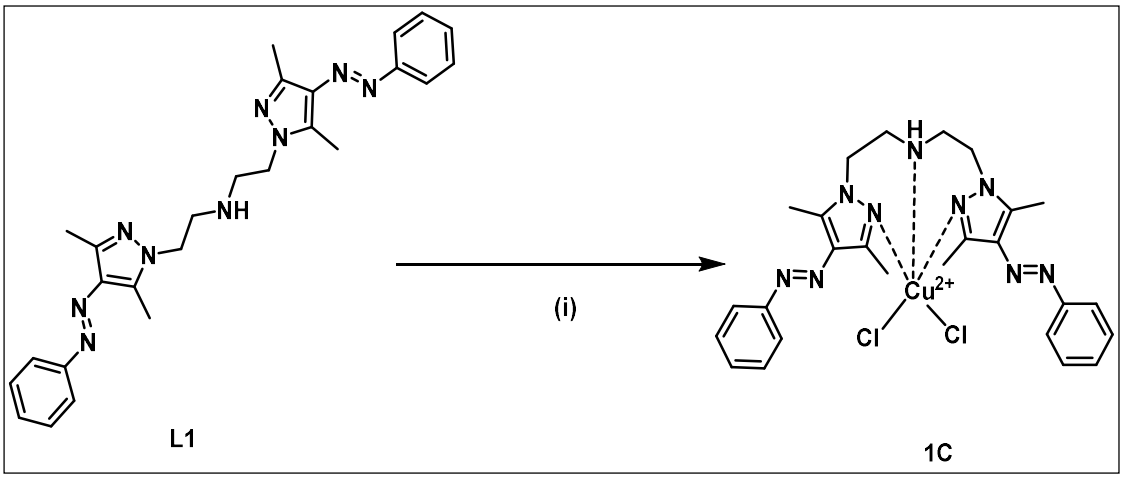

Scheme 2.10. Synthetic Scheme of Metal coordination complex **1C.** (i) $CuCl_2.2H_2O$, CH_3OH, rt, overnight, 77%.

2.4.2. Synthesis of metal coordination complexes with photo-active ligand L2

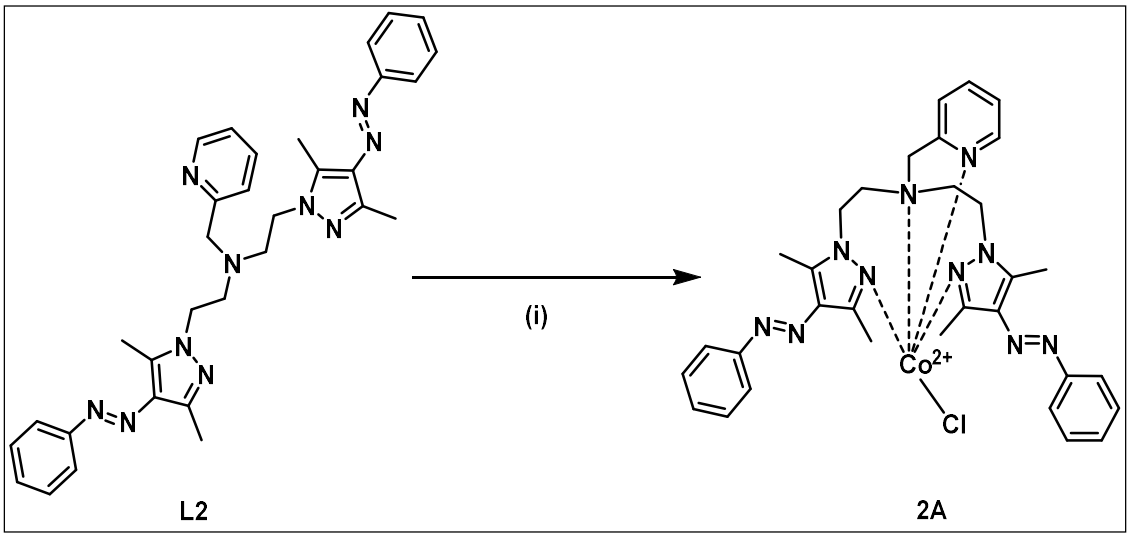

Scheme 2.11. Synthetic Scheme of Metal coordination complex **2A.** (i) $CoCl_2.6H_2O$, NH_4PF_6, CH_3OH, rt, overnight, 67%.

The coordination complexes of L2 were synthesized with cobalt chloride hexahydrate and copper chloride hexahydrate. The synthesis schemes for the coordination of the metal salts with photo-active ligand **L2** are given in Scheme 2.11-2.12. These synthesis strategies have been adapted from similar ones reported in literature[19]. The product was run through celite and then allowed to stand at room temperature. The crystals were collected by filtration, washed with ether and dried in air. The product

was confirmed by HRMS and kept for crystallization in CH_3CN, MeOH and 1:1 MeCN: MeOH.

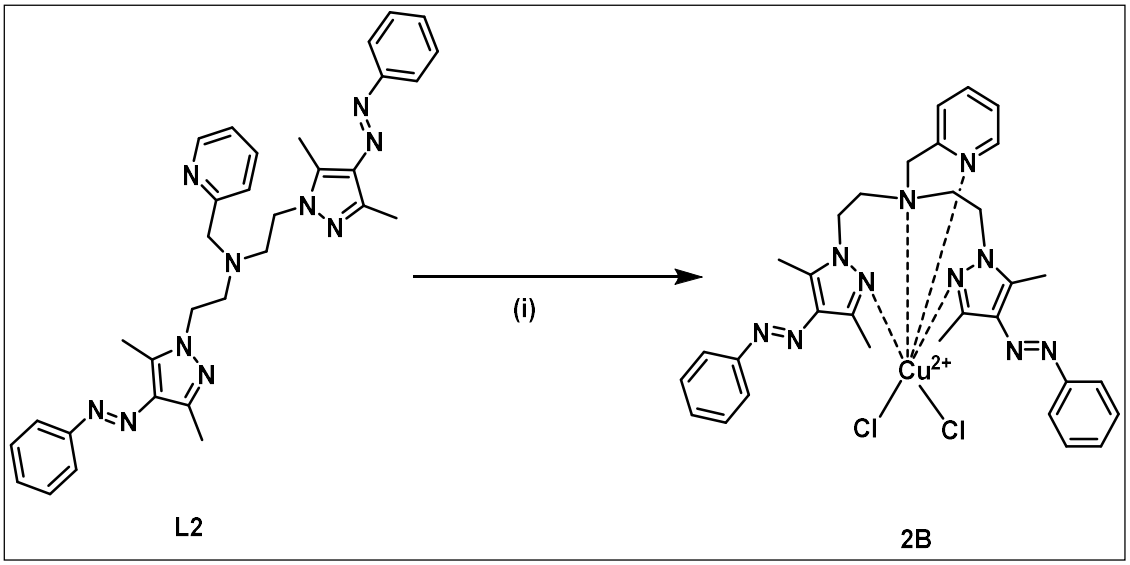

Scheme 2.12. Synthetic Scheme of Metal coordination complex **2B.** (i) $CuCl_2.2H_2O$, NH_4PF_6, CH_3OH, rt, overnight, 65%.

2.5. Photoswitching studies

The photoswitching behaviour of ligands **L1**-**L3** were investigated by UV and NMR spectroscopy. The difference in photoswitching behaviour of the ligands from that of their transition metal complexes was also thoroughly investigated.

2.5.1. Photoswitching studies of ligand L1

Analysis of photoswitching experiments were performed using UV-vis spectroscopy. In the figure 2.1, the blue line depicts the *trans* spectrum of target ligand **L1** in methanol having a maximum at 328 nm, which corresponds to the π-π* band of the azo group. The other maxima at 421 nm corresponding to the n-π* band has been observed as a weak absorption. The sample was irradiated with 365 nm for about two minutes to convert it to the *cis* form. Upon irradiation, there is blue shift in the wavelength of the π-π* absorption maxima to 298 nm along with a characteristic decrease in the intensity (red line). However, in contrast to the π-π* band, the n-π* band absorption intensity shows an increase indicating the formation of *cis* isomer. The n-π* band also shows a red shift in the absorption maxima, with the new maxima at 437 nm. Even after prolonged irradiation of the sample with 365 nm light, no other

change in the spectra was observed, which indicates the attainment of photostationary state. Now irradiation of the sample with a light of frequency within the n-π* band should bring the sample back to *trans*- state. The sample was irradiated with 505 nm light for 35 mins, upon which the π-π* band regained its absorbance intensity along with the reduction in the absorption intensity of n-π* band, confirming the reverse isomerisation of the sample. These observations conclusively confirm that the molecule underwent near complete photoswitching.

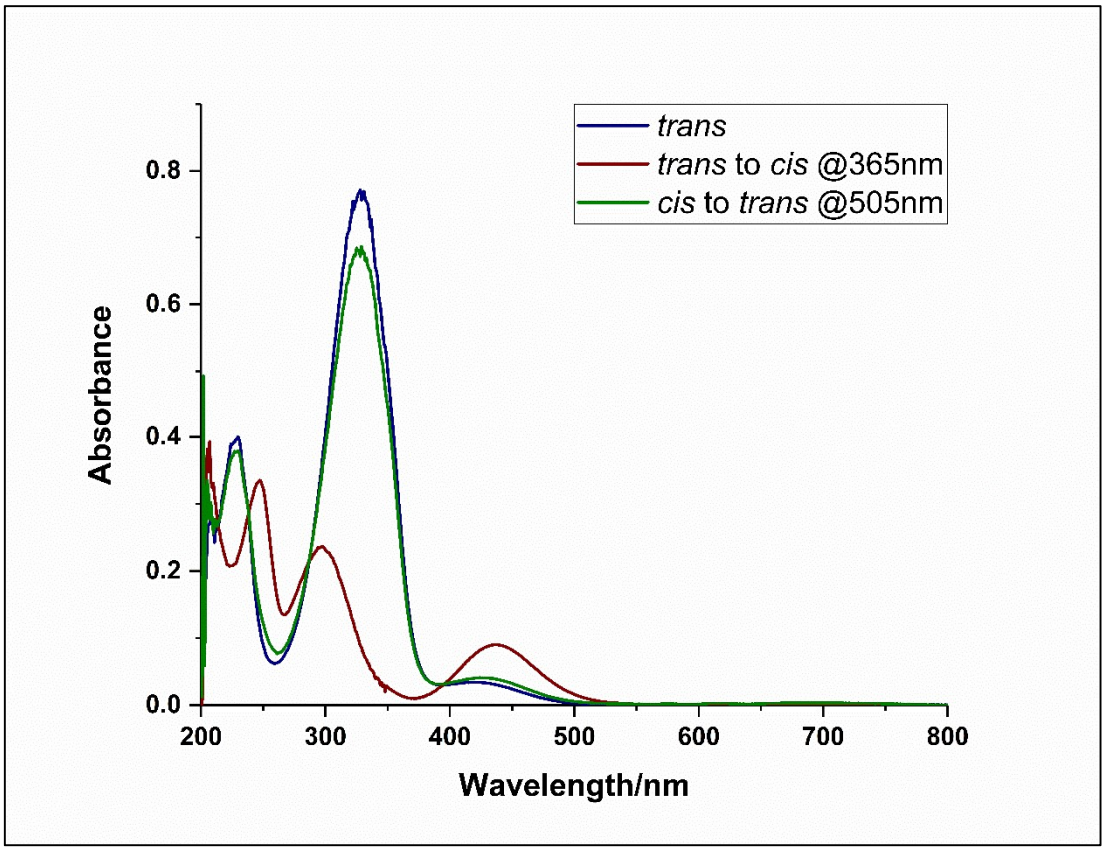

Fig 2.1. Analysis of solution phase photoswitching of **L1** using UV-vis spectroscopy (Solvent: CH_3OH; concentration: 59.6 $x10^{-5}$ M)

We had also performed solid state photoswitching studies on the ligand. Figure 2.2, shows the photoswitching of ligand in solid state (KBr). The blue line in the graph is indicative of the absorption spectra of the sample in its *trans*-form, which we can infer by the large absorption intensity at the π-π* band, and the lower absorption maxima at n-π* band. Upon irradiation with 365 nm light for around 5 mins, the sample undergoes forward switching to its *cis*-form (brown line). In its *cis*- form, n-π* band has a stronger intensity compared to that of *trans*-form. Also, upon reverse isomerisation with 505 nm light, the absorption intensity of n-π* band drops with an

increase to the π-π* band. Thus, we can confirm that the sample undergoes near cpmplete photoswitching

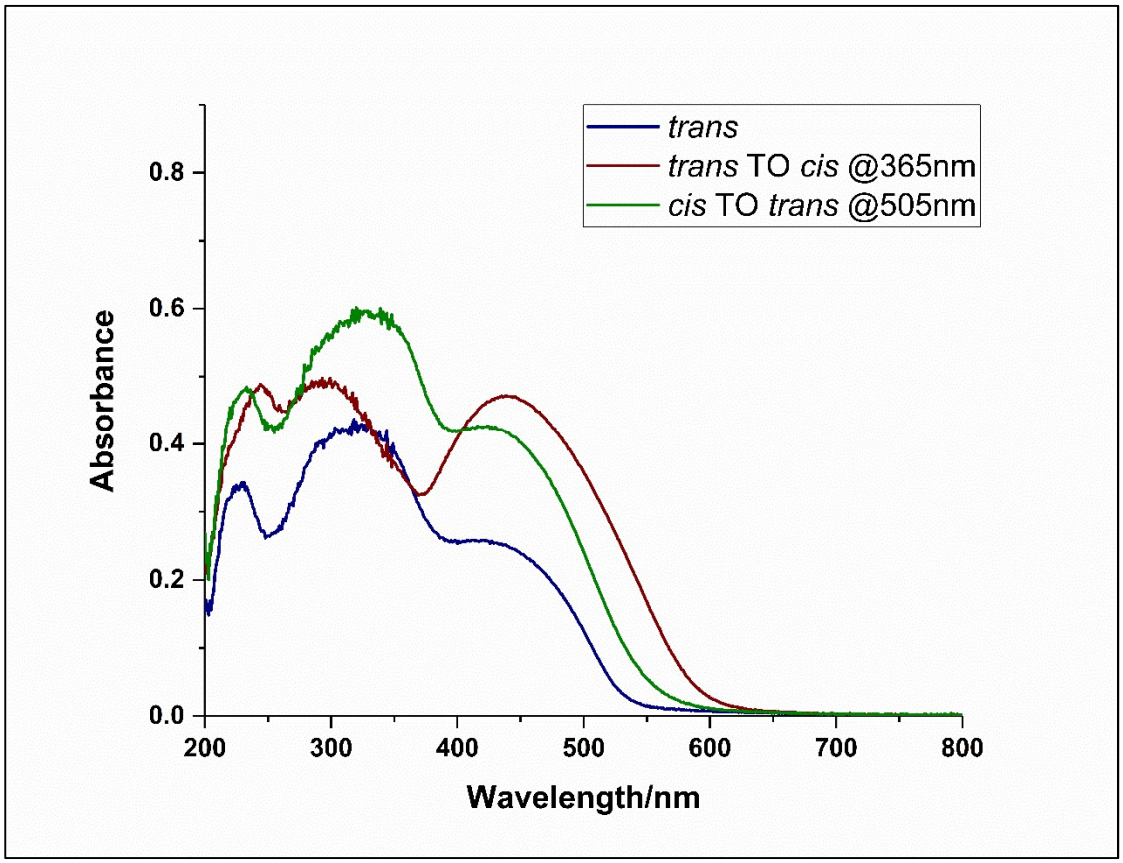

Fig 2.2. Analysis of Solid State Photoswitching studies of **L1** using UV-vis Spectroscopy (Medium: KBr)

Analysis of photoswitching experiments were also performed using ^{1}H NMR spectroscopy. In the figure 2.3, we have stacked the NMR spectrum of Ligand **L1** in its *trans* state, PSS after 365 nm irradiation and PSS after 505 nm irradiation (from bottom to top) in $CDCl_3$ solution. In the figure, we have highlighted the peaks corresponding to methyl protons of the pyrazole, because the shift of methyl peaks can be used to quantify and keep track of the forward or the backward photoisomerization. Upon forward isomerisation, due to the change in ring current in the *cis* form of the ligand, we can observe that the highlighted peak becomes deshielded. Upon irradiation at 505 nm, the sample undergoes reverse isomerisation to its *trans*-form. However, the isomerisation is not quantitative, as we can observe peaks corresponding to both the isomers in the spectrum. On integration of these peaks, we observed that in the photostationary state, the sample has around 86 % *trans* and 14 % *cis* isomer.

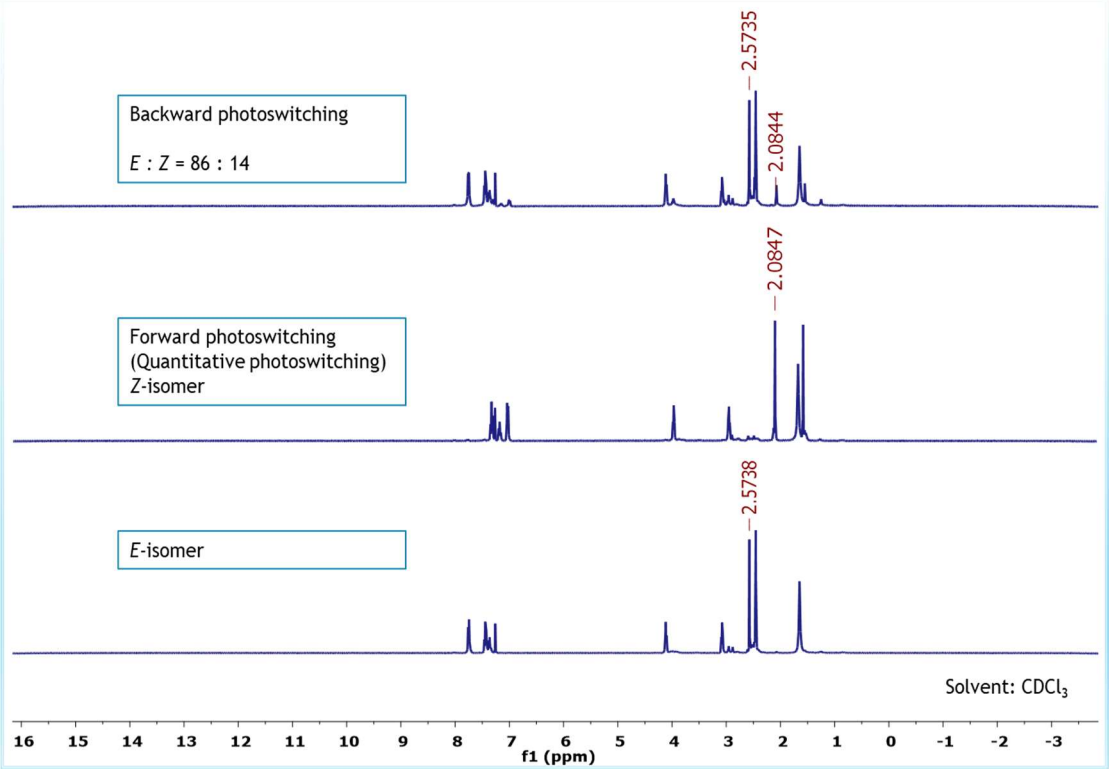

Fig 2.3. Analysis of photoswitching experiments using NMR spectroscopy in **L1** (Solvent: $CDCl_3$, concentration 17.83 mM)

2.5.2. Photoswitching studies of ligand L2

A similar studies have been carried out for the ligand **L2** as well. Figure 2.4 shows the photoswitching of target ligand **L2**. In the figure, the blue line shows the target ligand **L2** in its thermodynamically stable *trans*-form in methanol solution. Similar to ligand **L1**, the sample, undergoes isomerisation to *cis*- form upon irradiation with 365 nm light for 5 mins, which we can understand by the reduction in the intensity of the π-π* band along with the concurrent increase in the intensity of n-π* band. Also, upon forward switching, the wavelength of the absorption maxima of π-π* band undergoes a blue shift (282 nm from 319 nm) in its *trans*-state. Consecutively, the n-π* band exhibits a slight red shift in the absorption maxima from 418 nm to 423 nm. Upon prolonged irradiation of the sample with 365 nm light, there was no significant change in the spectrum indicating the attainment of photostationary state. The sample was reverse isomerised by irradiation with 490 nm light for 20 mins. Backward switching was confirmed by the regaining of the π-π* absorption intensity along with the drop in absorption intensity of the n-π* band. These observations helped us confirm that the molecule underwent near complete photoswitching.

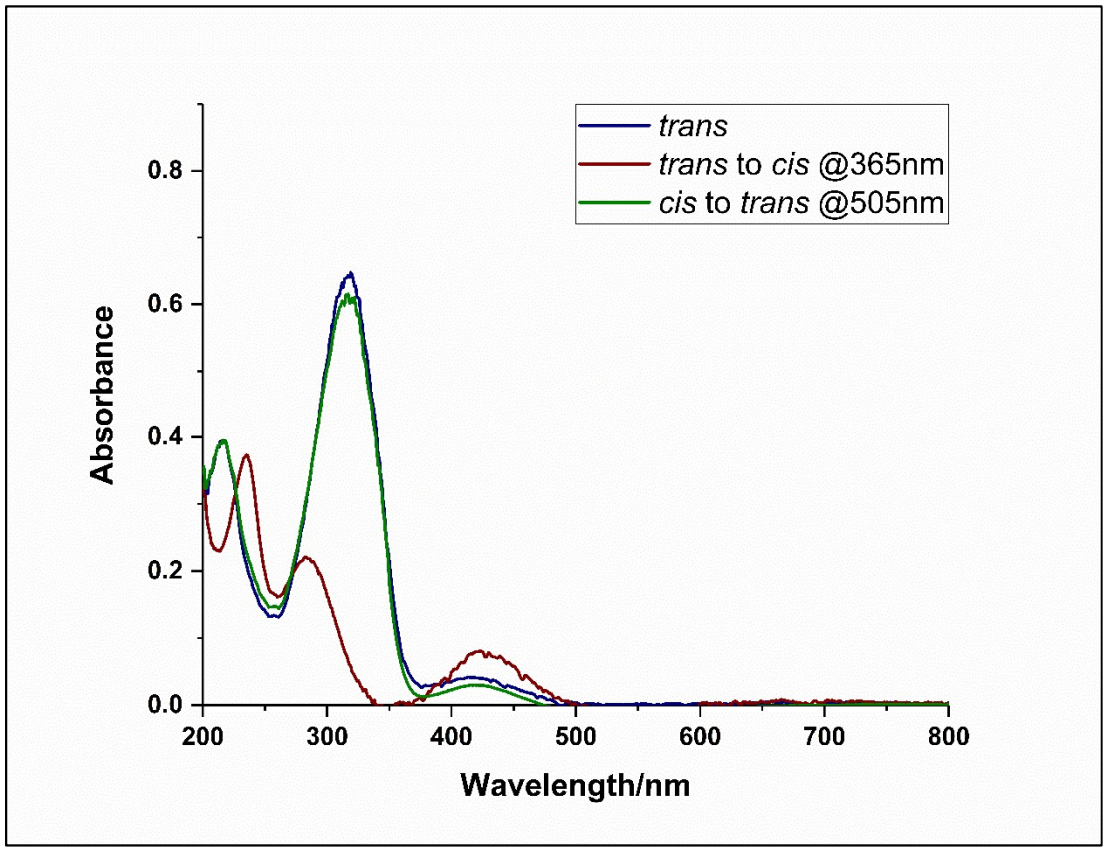

Fig 2.4. Analysis of photoswitching studies using UV-vis spectroscopy of **L2**.
(Solvent: CH_3OH; Concentration: 51.72 $x10^{-5}$M)

1H NM photoswitching studies were performed on the sample using NMR spectrometer. In the figure 2.5, we have stacked the NMR spectrum of the sample in its *trans*-form, the PSS after 365 nm irradiation, and PSS after 490 nm irradiation on top of the other. In the figure, the protons of one of the methyl groups is highlighted upon isomerisation. On forward switching, the protons become less shielded due to change in the ring current of pyrazole unit. On reverse isomerisation, we can observe two peaks corresponding to the same protons, which shows us that reverse isomerisation is not quantitative. Integration of these peaks showed us that in the photostationary state, 82 % of the sample is in *trans* - form while the rest is in *cis*-state. Thus these studies also help us confirm that the sample undergoes near complete photoswitching.

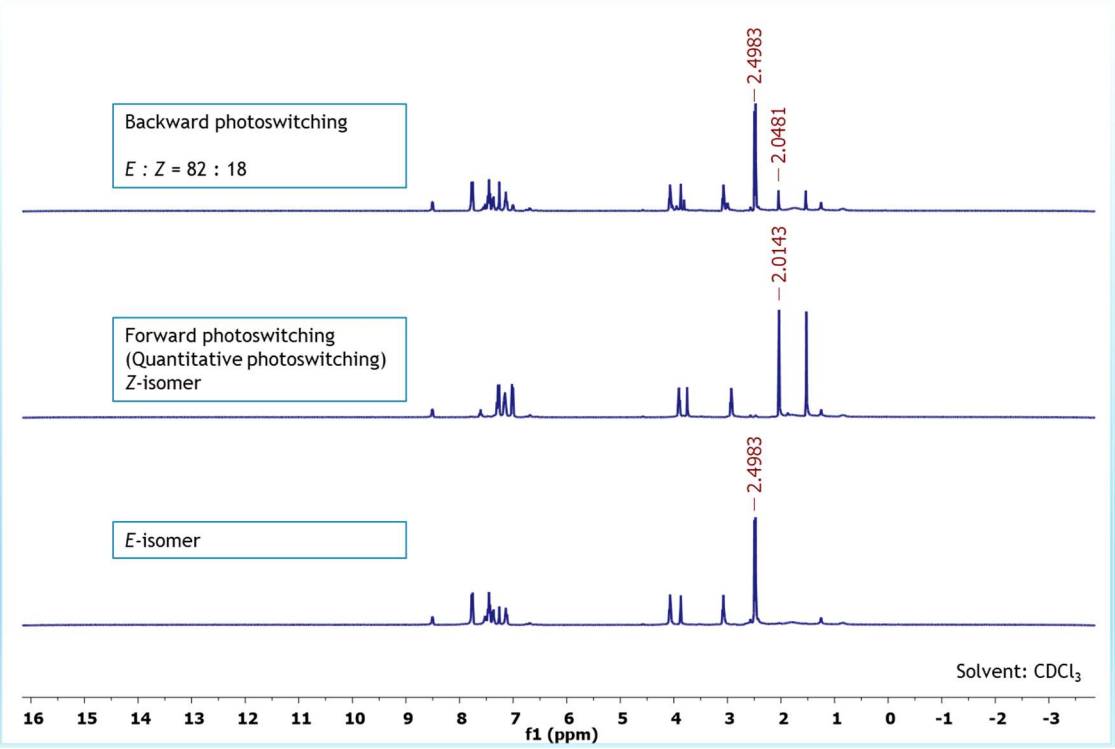

Fig 2.5. Analysis of NMR photoswitching studies of **L2** using ^{1}H NMR Spectroscopy (Solvent: $CDCl_3$; Concentration: 21.29 mM)

2.5.3. Photoswitching studies of metal complex 1A

The photoswitching behaviour of metal complex **1A** is very similar to that of its ligand molecule **L1**. However, the absorption features are slightly blue shifted in the case of the metal complex compared to the ligand. UV photoswitching experiment was performed using UV spectrophotometer. Figure 2.6, shows the photoswitching behaviour of **1A** in methanol solution. The blue line depicts the absorption spectrum of the sample in its tans- form. Just like in the parent molecule, on forward switching with 365 nm light, the absorption intensity of π-π* band decreases, while the absorption intensity of n-π* band increases. Also, on reverse isomerisation at 490 nm, the spectrum regains its characteristics as shown by the *trans*-isomer. All of these observations, help us confirm that the sample undergoes near complete photoisomerization.

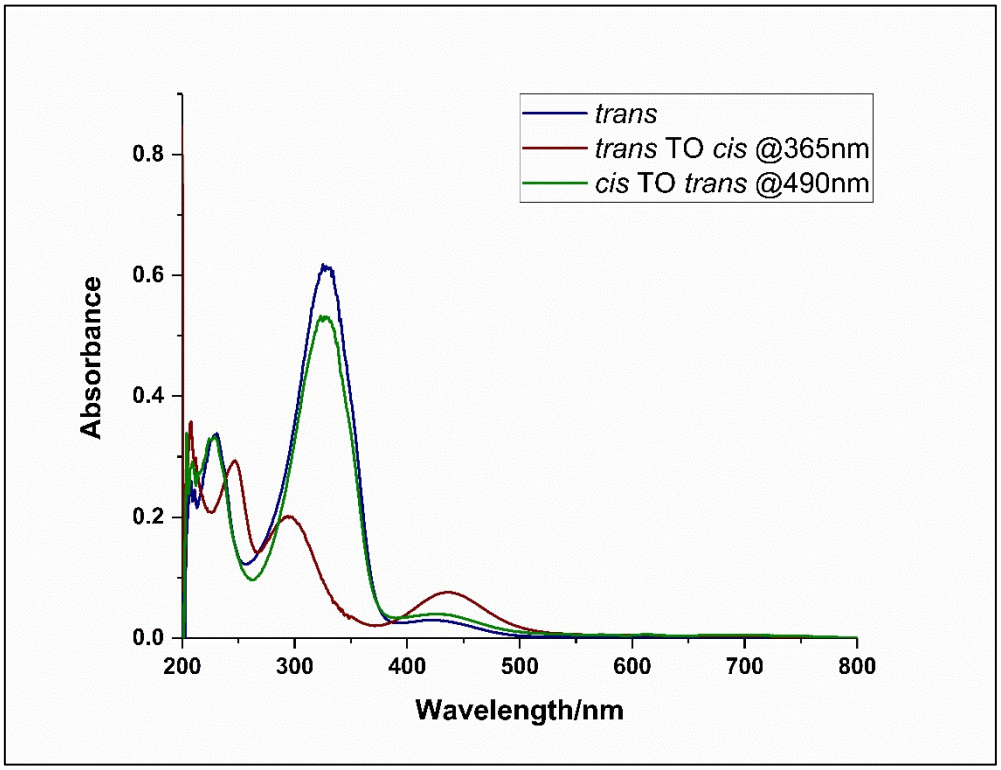

Fig 2.6. Analysis of photoswitching studies of **1A** using UV-vis spectroscopy. (Solvent: Methanol; Concentration: 70.09 x10^{-5} M)

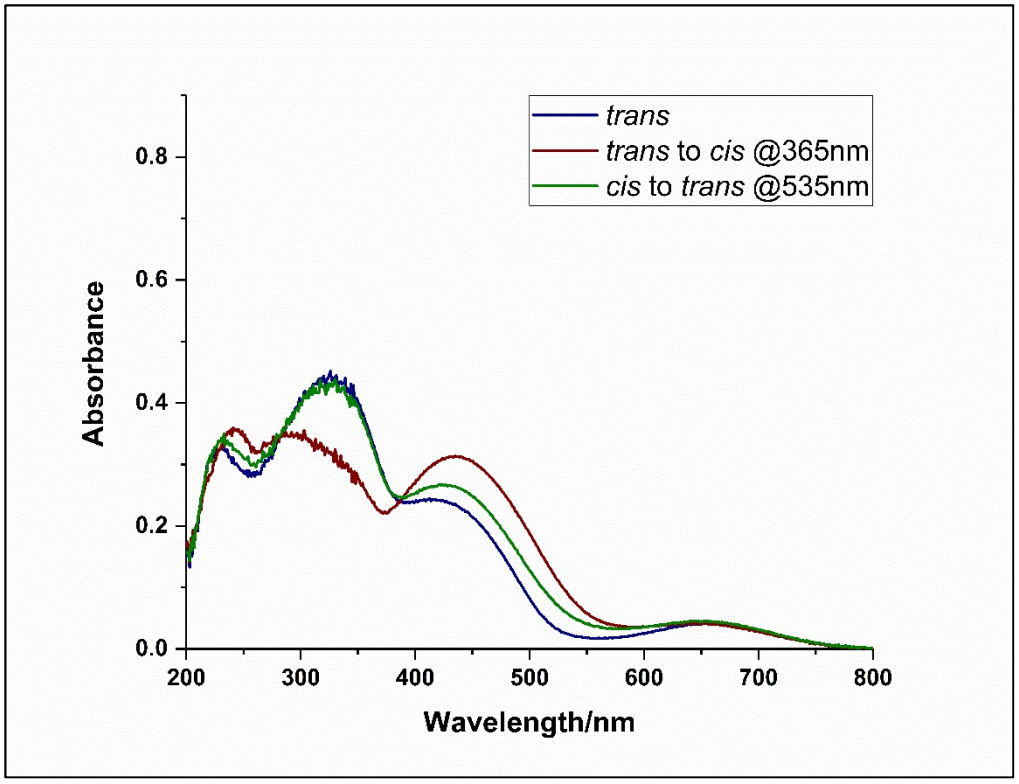

Fig 2.7. Analysis of solid state photoswitching studies of **1A** using UV-vis spectroscopy. (Medium: KBr)

The same experiment was repeated in the solid state of the metal complex in KBr. The absorption features of the metal complex was similar to that those observed for the parent ligand **L1**. In addition to the absorption bands belonging to π-π* and n-π* bands, we have also observed a new band arising at around 650 nm, which we believe is due to ligand to metal charge transfer (LMCT) effects.

2.5.4. Photoswitching studies of metal coordination complexes 1B and 1C

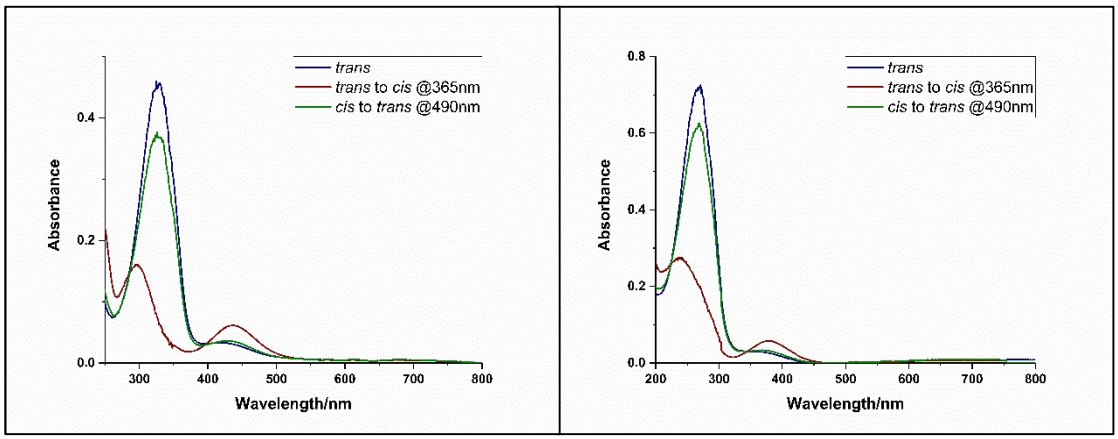

Fig 2.8. Analysis of photoswitching studies of (a) Co(II) complex **1B** (Solvent: Methanol; Concentration: 96.75 x10^{-5} M); (b) Cu(II) complex **1C** (Solvent: Methanol; Concentration: 87.41 x10^{-5} M) using UV-vis spectroscopy.

Photoswitching studies of metal coordination complexes **1B** and **1C** were performed using UV spectrometer in methanol solution. The photoswitching aspects of these complexes were like that of complex **1A**. The absorption maxima are slightly blue shifted compared to the parent ligand. No other anomalies were observed. We were able to confirm that the complexes underwent partial photoswitching from these experiments.

2.6. Photo physical studies

We tried to investigate the changes in the spectral features that were brought by the coordination of transition metals to target photo-active ligands. In the figure 2.9, we have superimposed the UV absorption spectrum of the ligand **L1** along with the spectra of its corresponding metal complexes. From the figure, we can see that the basic spectral features like the high intensity π-π* band and low intensity n-π* bands

have been replicated in the metal complexes. However, the frequency at which maximum absorption happens, have been blue shifted compared to that of the parent ligand. Though this effect is not apparent in the case of Ni complex (**1A**) and Cobalt complex (**1B**), there is considerable blue shift in the case of Copper complex (**1C**). The blue shift in the absorption frequency is indicative of an increase in the π-π* band gap. Possible reasons can be a selective stabilisation of the HOMO by the delocalisation of the electrons with the metal centre or destabilization of the LUMO upon coordination.

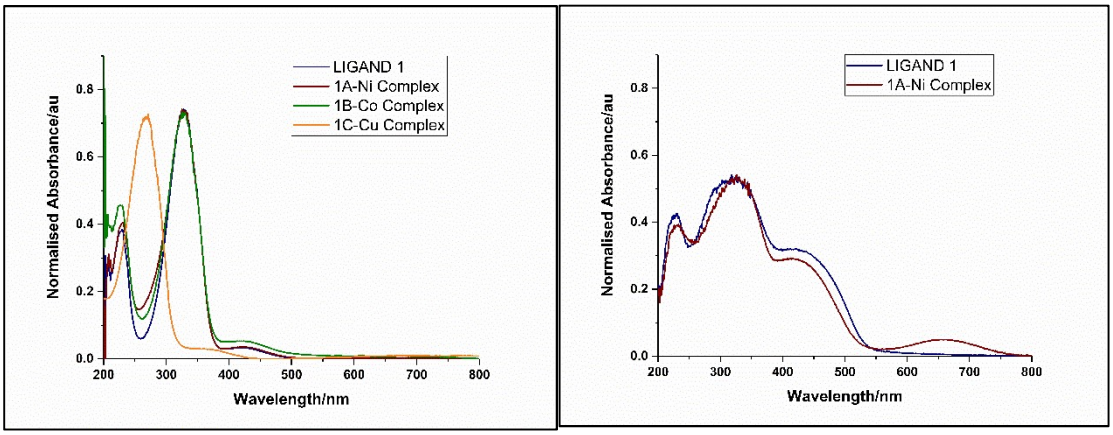

Fig 2.9. Solution phase UV-vis absorption spectra of metal complexes superimposed with spectra of **L1** in methanol. (Normalized absorption); Solid state UV absorption spectra of **L1** and **1A** in KBr medium.

We had also investigated the changes in the spectrum in the solid state. In the figure 2.9, we have superimposed the *trans*-isomer absorption spectra of the parent ligand **L1** and Nickel complex **1A**. In solid state, there is no significant change in the π-π* and n-π* absorption bands. However, around the 650 nm range, we start to observe a new band, which we contemplate to belong to the ligand to metal charge transfer (LMCT) band. Moreover, on investigating the melting point of the ligand and the metal complexes, we have observed a significant increase in the melting point of the metal complexes that indicates a tuning of the physical properties of the complexes upon coordination with metal centre.

Name	λmax $(\pi - \pi^*)$ (nm)	λmax $(n-\pi^*)$ (nm)	Melting Point (°C)
LIGAND 1	328	421	84
Ni Complex	325	421	182
Co Complex	325	424	190
Cu Complex	271	358	170

Table 2.1. Absorption of Maxima and melting point of L1 and its Metal coordination complexes

2.7. Photochromism

Photochromism is the reversible transformation of a species between two or more isomeric forms upon irradiation with an electromagnetic radiation, where each form has different absorption spectra. That is, they should show a change in colour upon photoswitching. We had designed our photo-active ligands such that they show photochromism in both solid and liquid phases. In figures 2.10-2.11, we have tried to elucidate the photochromic behaviour of our target ligand **L1** in different medium. One peculiar observation that we had made towards the photoisomerisation of ligand **L1** in solid state is that it starts to melt when isomerised to its *cis*- isomer. This phenomena is called light induced phase transition, i.e. upon photoisomerisation, the physical properties are affected so as to induce phase transition in the molecule.

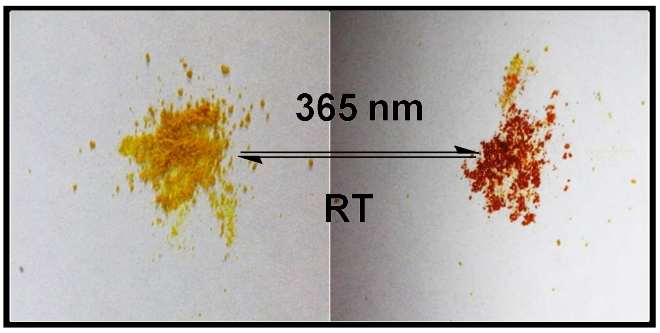

Fig 2.10. Photochromic activity of target ligand **L1** in solid state

Fig 2.11. Photochromic activity of target ligand **L1** in methanol solution.

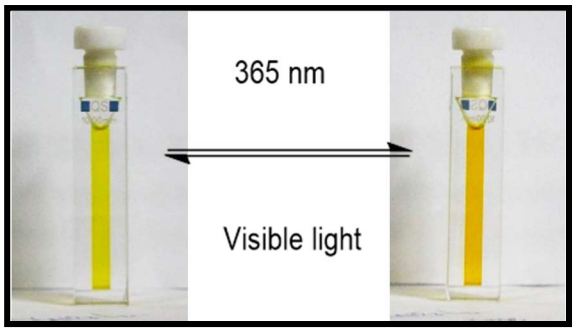

Concurrently, photochromism was also observed in the metal complexes synthesised from these ligands. However, the colours of the metal complexes could be tuned by varying the transition metal that is coordinated to the chelating centres.

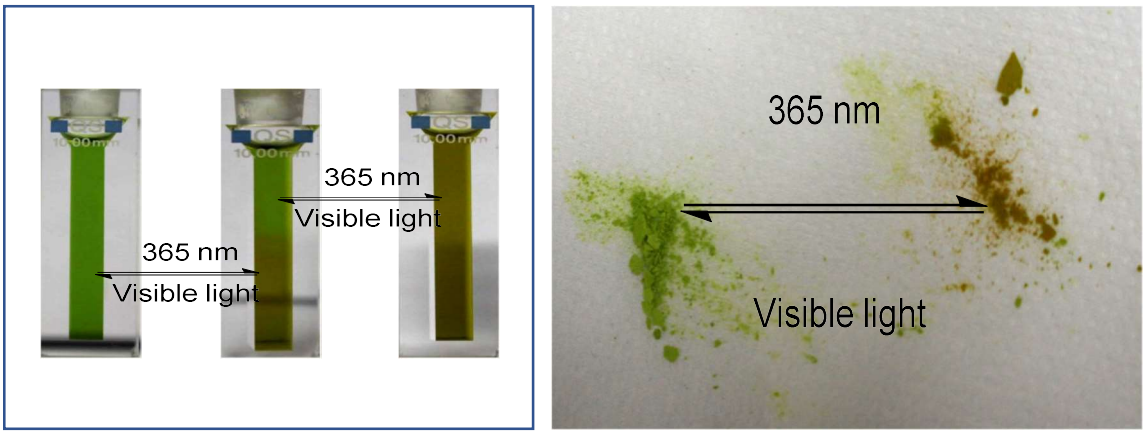

Fig 2.12. Photochromism of Complex **1A** in methanol solution (left) and Solid state (right)

2.8. Crystal structure

Crystallisation was attempted for all the metal complexes synthesised. Interestingly, we were able to obtain a single crystal XRD data for target **complex 2B** (slow evaporation in acetonitrile). x-ray quality crystals of **2B** were obtained by keeping it in acetonitrile solution at 4 °C. The single crystal X-ray structure of **2B** shows that this complex crystallizes in the triclinic system with the *P-1* space group. The counter anion hexafluorophosphate is also present in the unit cell along with acetonitrile, which was the solvent of crystallization. The geometry around central metal atom is distorted square pyramidal.

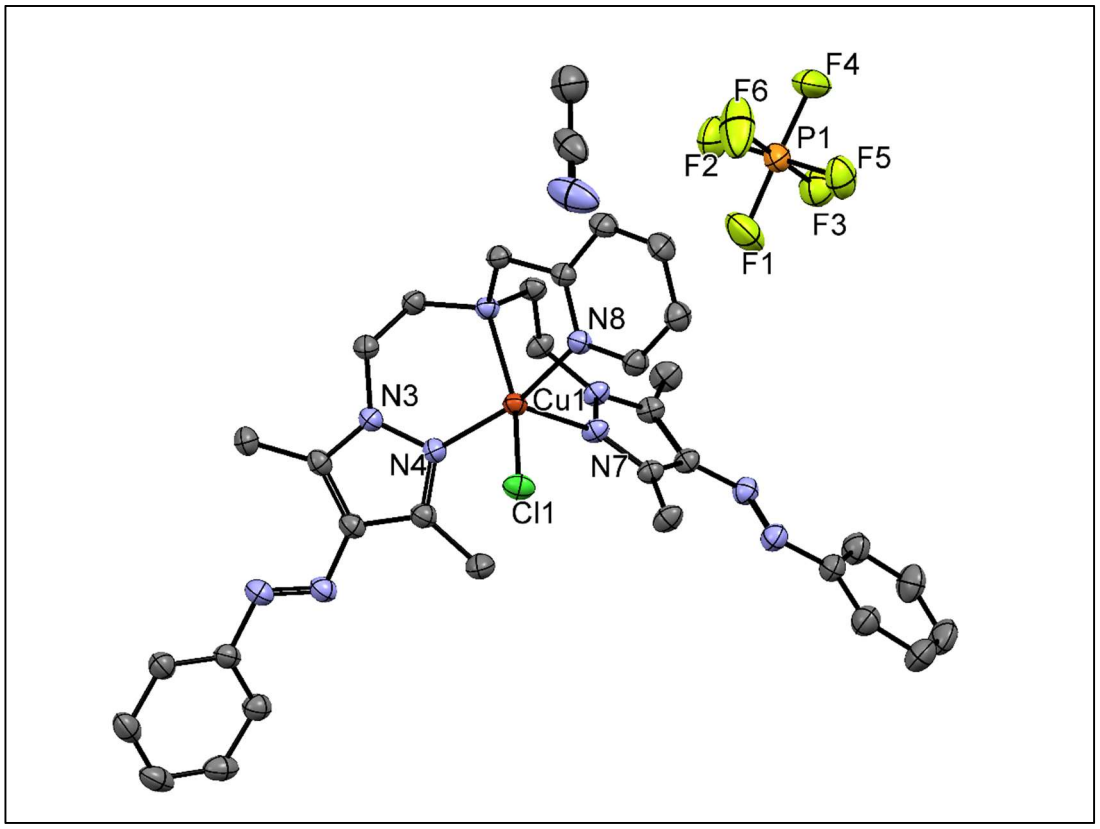

Fig 2.13. Single crystal x-ray structure of **2B.** All Hydrogen atoms have been omitted for clarity. Selected bond lengths [**Å**] and bond angles [^{0}]: Cu1-Cl1 2.277, Cu1-N4 2.008, Cu1-N7 2.260, Cu1-N8 2.012, Cu1-N5 2.118, N4-Cu1-N5 90.95, N7-Cu1-N5 95.74, N8-Cu1-N5 80.55.We had also collected PXRD data for other metal complexes.

2.8.1. Photoswitching experiments with crystals of 2B

Photoswitching experiment was done on **2B** crystals using NMR spectrometer in acetonitrile solution. Given below (Fig 2.14; red spectrum) is the NMR spectrum of the acetonitrile solution of the crystal in its thermodynamically stable *trans*-state.

Upon irradiation of the crystal solution with 365 nm light for about 5 minutes, there is a visible change in colour indicating photochromism in the sample. The NMR spectrum of the sample in its *cis*- state was recorded and is shown below (Fig 2.1; blue spectrum).

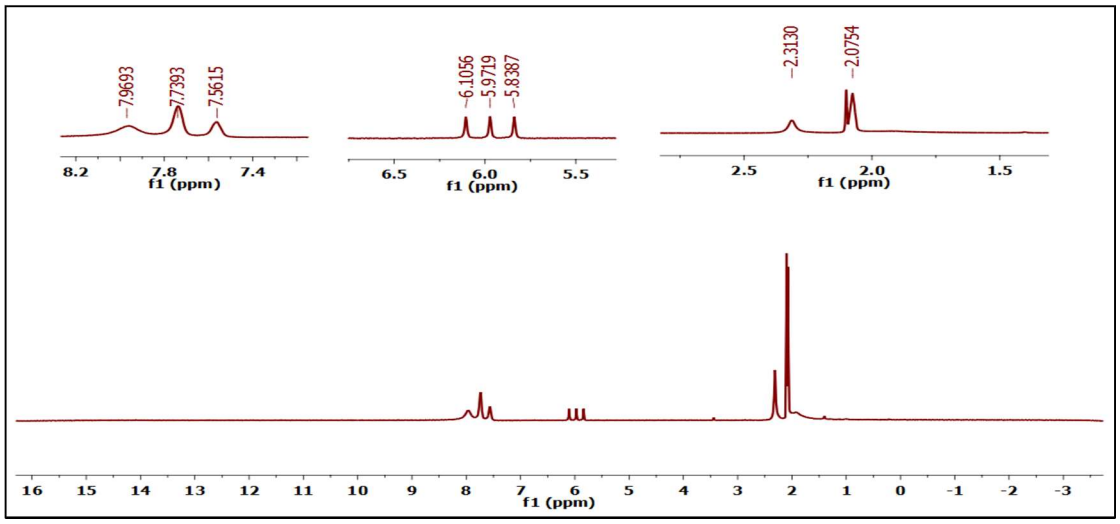

Fig 2.14. NMR spectrum of **2B** (*trans* isomer). (All peaks zoomed in on top; Solvent: CH_3CN; Concentration: 15.26 mM)

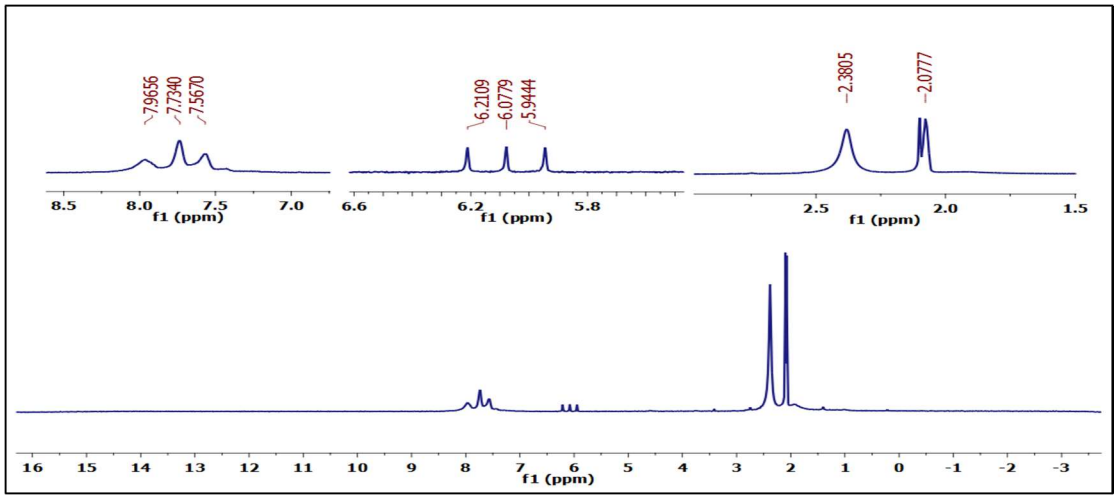

Fig 2.15. NMR spectrum of **2B** (*cis* isomer). (All peaks zoomed in on top; Solvent: CH_3CN; Concentration: 15.26 mM))

The peaks from the *trans* (red line) isomer and *cis* (turquoise line) isomer has been superimposed in the figure given below (Fig. 2.16). The shielding of the proton peaks in what appears to be the CH_2 protons of the ligand unit is an indicative of photoswitching of the sample.

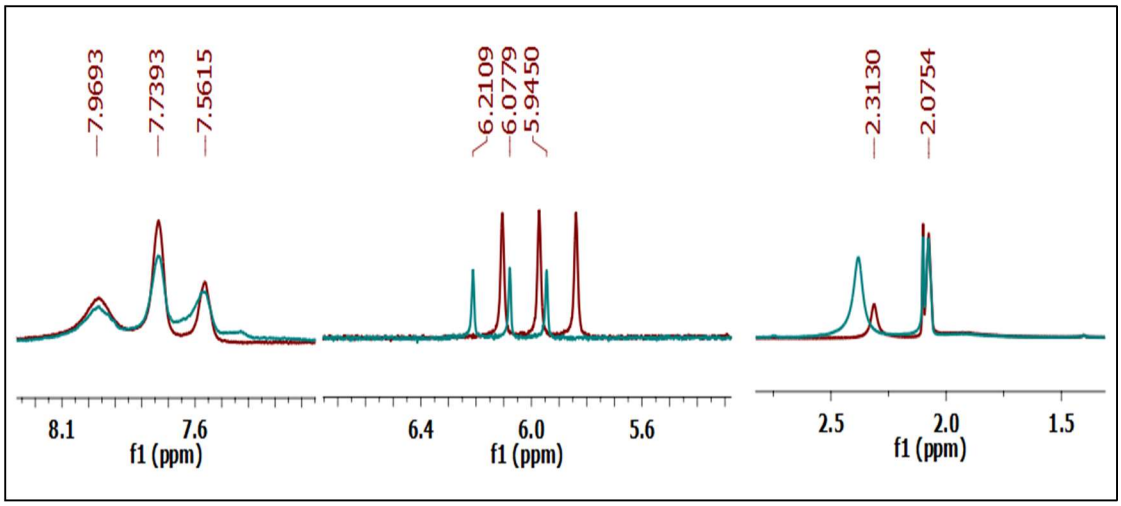

Fig 2.16. Superimposed NMR spectra of **2B** in *trans* (red) and *cis* (turquoise) form

Chapter 3: Summary and outlook

NNN pincer type pyrazole based ligands were chosen as our photoresponsive targets. All the designed targets have been synthesized successfully and fully characterized. Using different metal salts, coordination complexes of Cu(II), Co(II) and Ni(II) have been made. The UV-vis absorption properties, photoswitching behaviour and melting points have been compared with the free ligands. Also, using HRMS data, the formation of the complexes have been confirmed. For one of the complexes, we have confirmed the structure using single crystal XRD. The photoswitching behaviour is solution and solid phase exhibited a very interesting photochromism. Attempts on crystallizing the remaining complexes, and understanding the photochromism are currently underway. These complexes can be potential lead for controlling various properties like magnetic and colour as well as light-driven catalysis.

Chapter 4: Materials and methods

4.1. General methods and instrumentation

All the commercially available chemicals were purchased from Sigma Aldrich, HiMedia, Merck, TCI and Avra. Progress of reactions was monitored using prepared TLC and detected using UV (254 nm and 365 nm), $KMnO_4$ and Iodine. Organic extracts were dried using commercially available anhydrous sodium sulphate and the solvent was removed by rotary evaporation (Buchi). Separation and purification was done by column chromatography using Silica-Gel (100-200 and 60-120 mesh size) purchased from HiMedia. LED of different wavelength were purchased from Applied Photophysics. ^{1}H and ^{13}C NMR were recorded in Bruker Avance-III 400 MHz and 100 MHz spectrometers with trimethylsilane as standard using $CDCl_3$/DMSO-d_6 as solvent, corresponding residual signals of $CDCl_3$ and DMSO-d_6 are 7.62 ppm and 2.50 ppm respectively. Chemical shift values were recorded in ppm scale. IR spectra were recorded in KBr plate or thin film or Perkin-Elmer FT-IR spectrometer and Bruker Alpha IR spectrophotometer. HRMS was recorded in both ESI positive and negative modes using Waters SYNAPT G25 High definition mass spectrometer. UV-Vis Spectroscopy for photoswitching was done using Agilent spectrophotometer.

4.2. Synthesis

4.2.1. Synthesis of bis(2-(3,5-dimethyl-4-((*E*)-phenyldiazenyl)-1H-pyrazol-1-yl)ethyl)amine (L1)

To a round bottom flask containing NaH (60 mg, 1.5 mmol) in dry DMF (0.6 mL), a solution of 3,5-dimethyl-4-(phenyldiazenyl)-1H-pyrazole (300.26 mg, 1.5 mmol) in dry DMF (0.5 mL) was added dropwise. The reaction mixture was stirred for 2 hours at room temperature. Then a solution of bis (2-chloroethyl) amine hydrochloride (89.24 mg, 0.5 mmol) in dry DMF (0.3 mL) was added dropwise to mixture. The mixture was further stirred for 2 hours at 70 ^{O}C. The resulting residue was extracted with DCM, washed with water, followed by addition of anhydrous sodium sulphate. Volatiles were removed under reduced pressure and the product was isolated by silica-gel column chromatography(ethyl acetate as eluent).

^{1}H NMR (400 MHz, $CDCl_3$) δ (ppm): 2.4543 (s, 6H), 2.719 (s, 6H), 3.0736 (t, J=5.92 Hz, 4H), 4.1167 (t, J=5.92 Hz, 4H), 4.7696 (s, 1H), 7.3621 (t, J=8.28 Hz, 4H), 7.4435 (t, J=7.8 Hz, 4H), 7.7426 (d, J=7.24 Hz, 2H); ^{13}C NMR (100 MHz, $CDCl_3$) δ (ppm): 9.8905, 14.0103, 48.6936, 48.7337, 76.7721, 77.0397, 77.3574, 121.7633, 128.8757, 129.3068, 135.0053, 139.2140, 142.7530, 153.5697; HRMS TOF MS ESI+ Theoretical m/z: 470.2781, Observed m/z: 470.2908

4.2.2. Synthesis of 2-(3,5-dimethyl-4-((*E*)-phenyldiazenyl)-1H-pyrazol-1-yl)-N-(2-(3,5-dimethyl-4-((*E*)-phenyldiazenyl)-1H-pyrazol-1-yl)ethyl)-N-(pyridin-2-ylmethyl)ethan-1-amine (L2)

A mixture of bis(2-(3,5-dimethyl-4-((*E*)-phenyldiazenyl)-1H-pyrazol-1-yl)ethyl)amine-(L1) (1 g, 2.11 mmol), 2 (Chloro methyl) pyridine hydrochloride (348.905 mg, 2.11 mmol) and anhydrous K_2CO_3 (735.09mg, 3.32mmol) was suspended in dry CH_3CN. The resulting mixture was stirred and refluxed gently under N_2 gas for 3 days, during which colour turns yellowish brown. The reaction mixture was the cooled in ice, unreacted KCl and K_2CO_3 was filtered off .Solvent was removed under reduced pressure. The resulting residue was extracted with DCM, washed with water and brine and followed by addition of anhydrous sodium sulphate. Volatiles were removed under reduced pressure and the product was isolated using silica-gel chromatography. (Ethyl acetate)

^{1}H NMR (400 MHz, $CDCl_3$) δ (ppm): 2.4782 (d, J=7.48 Hz, 12H), 3.0750 (t, J=6.56 Hz, 4H), 3.8704 (s, 2H), 4.0713 (t, J=6.52 Hz, 4H), 7.364 (t, J=7.36 Hz, 2H), 7.3648 (t, J=7.24 Hz, 2H), 7.4503 (t, J=7.84 Hz, 4H), 7.7557 (d, J=7.32 Hz, 4H), 8.5092 (d, J=4.36 MHz, 1H); ^{13}C NMR (100 MHz, $CDCl_3$) δ (ppm): 9.9714, 14.1193, 47.3500, 54.1902, 60.8609, 122.8823, 122.3736, 122.9697, 129.0126, 129.4235, 135.1915, 136.6942, 139.2207, 142.6968, 149.1975, 153.7174, 158.8306; HRMS TOF MS ESI+ Theoretical m/z: 561.3203, Observed m/z: 561.32332.

4.2.3. Synthesis of N,N-bis(2-(3,5-dimethyl-4-((*E*)-phenyldiazenyl)-1H-pyrazol-1-yl)ethyl)prop-2-yn-1-amine (P2)

Bis(2-(3,5-dimethyl-4-((*E*)-phenyldiazenyl)-1H-pyrazol-1-yl)ethyl)amine-(L1) (23.822mg, 0.5mmol) was dissolved in CH_3CN (1.2 mL), to which K_2CO_3 (277.01 mg, 2 mmol) was added and then 3-bromopropyne (80 % w/w in toluene, 0.0481 mL, 0.54 mmol) was added dropwise. The resulting yellow suspension was refluxed overnight, over which it became dark brown in colour. K_2CO_3 was filtered off and the resulting dark brown solution was run through a plug of basic alumina. Volatiles were removed under reduced pressure. The product could not be isolated by column chromatography. The crude mixture was brown oil.

HRMS TOF MS ESI+ Theoretical m/z: 508.2937, Observed m/z: 508.2618.

4.2.4. Synthesis of N-((1-benzyl-1H-1,2,3-triazol-5-yl)methyl)-2-(3,5-dimethyl-4-((*E*)-phenyldiazenyl)-1H-pyrazol-1-yl)-N-(2-(3,5-dimethyl-4-((*E*)-phenyldiazenyl)-1H-pyrazol-1-yl)ethyl)ethan-1-amine (L3)

Benzyl bromide (171.0370 mg, 0.107 mmol), NaN_3 (65.0099 mg, 0.1.7 mmol), $CuSO_4.5H_2O$ (149.69 mg, 0.039 mmol) and sodium ascorbate (198.11 mg, 0.097 mmol) were combined in DMF/H_2O (4:1, 1.5 mL). N,N-bis(2-(3,5-dimethyl-4-((*E*)-phenyldiazenyl)-1H-pyrazol-1-yl)ethyl)prop-2-yn-1-amine (507.646 mg, 0.098 mmol) was added to the reaction mixture and the resulting brown solution was stirred at room temperature for 24 hours. An aqueous solution of EDTA/ 1M NH_4OH (10 mL) was then added and the resulting solution was stirred at room temperature for 1 hour. The product was extracted with $CHCl_3$ and washed with water and brine. Anhydrous sodium sulphate was added. Volatiles were removed under reduced pressure. We tried to isolate the product using silica-gel column chromatography. But we were unable to isolate the product. The product however, was confirmed by HRMS.

HRMS TOF MS ESI+ Theoretical m/z: 641.3577, Observed m/z: 641.3620.

4.2.5. Synthesis of (1A)

To a solution of $NiCl_2.6H_2O$ (24 mg, 0.1 mmol) in MeOH (2 mL) a solution of Bis(2-(3,5-dimethyl-4-((*E*)-phenyldiazenyl)-1H-pyrazol-1-yl)ethyl)amine-(L1) (46.9 mg, 0.1 mmol) in THF (2 mL) was added and the resulting solution was stirred for 3 hours at room temperature. Volatiles were removed under educed pressure and the resulting green solid residue was washed with diethyl ether to afford an olive green solid. The product was confirmed by HRMS. Crystallisation of the complex was attempted by slow diffusion of hexane into saturated acetonitrile and methanol solutions of the product.

HRMS TOF MS ESI+ Theoretical m/z: 562.1733, Observed m/z: 562.11729

4.2.6. Synthesis of (1B)

To a solution of $CoCl_2.6H_2O$ (24 mg, 0.1 mmol) in MeOH (2 mL) a solution of Bis(2-(3,5-dimethyl-4-((*E*)-phenyldiazenyl)-1H-pyrazol-1-yl)ethyl)amine-(L1) (46.9 mg, 0.1 mmol) in THF (2 mL) was added and the resulting solution was stirred for 3 hours at room temperature. Volatiles were removed under educed pressure and the resulting green solid residue was washed with diethyl ether to afford a bright green solid. Crystallisation of the complex was attempted by slow diffusion of hexane into saturated acetonitrile and methanol solutions of the product.

4.2.7. Synthesis of (1C)

To a solution of $CuCl_2.2H_2O$ (17 mg, 0.1 mmol) in MeOH (2 mL) a solution of Bis(2-(3,5-dimethyl-4-((*E*)-phenyldiazenyl)-1H-pyrazol-1-yl)ethyl)amine-(L1) (46.9 mg, 0.1 mmol) in THF (2 mL) was added and the resulting solution was stirred for 3 hours at room temperature. Volatiles were removed under educed pressure and the resulting green solid residue was washed with diethyl ether to afford a dark green solid. The product was confirmed by HRMS. Crystallisation of the complex was attempted by slow diffusion of hexane into saturated acetonitrile and methanol solutions of the product.

HRMS TOF MS ESI+ Theoretical m/z: 532.2022, Observed m/z: 532.1987

4.2.8. Synthesis of (2A)

To 2-(3,5-dimethyl-4-((*E*)-phenyldiazenyl)-1H-pyrazol-1-yl)-N-(2-(3,5-dimethyl-4-((*E*)-phenyldiazenyl)-1H-pyrazol-1-yl)ethyl)-N-(pyridin-2-ylmethyl)ethan-1-amine (L2) (100 mg, 0.28 mmol) dissolved in MeOH (23 mL) , $CoCl_2.6H_2O$ (68.8 mg, 0.28 mmol) was added and the reaction mixture was heated for 10 minutes, followed by the addition of NH_4PF_6 (73.86 mg, 0.45 mmol). The resulting solution was run through celite and then allowed to stand at room temperature. After two days, the solid which were collected by filtration was washed with ether and dried in air. The product was confirmed by HRMS. Crystallisation of the complex was attempted by slow diffusion of hexane into saturated acetonitrile and methanol solutions of the product.

HRMS TOF MS ESI+ Theoretical m/z: 654.2134, Observed m/z: 654.2128

4.2.9. Synthesis of (2B)

To 2-(3,5-dimethyl-4-((*E*)-phenyldiazenyl)-1H-pyrazol-1-yl)-N-(2-(3,5-dimethyl-4-((*E*)-phenyldiazenyl)-1H-pyrazol-1-yl)ethyl)-N-(pyridin-2-ylmethyl)ethan-1-amine (L2) (100 mg, 0.28 mmol) dissolved in MeOH (23 mL) , $CuCl_2.2H_2O$ (70.6 mg, 0.28 mmol) was added and the reaction mixture was heated for 10 minutes, followed by the addition of NH_4PF_6 (73.86 mg, 0.45 mmol). The resulting solution was run through celite and then allowed to stand at room temperature. After two days, the solid which were collected by filtration was washed with ether and dried in air. The product was confirmed by HRMS. Crystallisation of the complex was attempted by slow diffusion of hexane into saturated acetonitrile and methanol solutions of the product.

HRMS TOF MS ESI+ Theoretical m/z: 658.2098, Observed m/z: 658.2119.

^{1}H NMR (400 MHz, $CDCl_3$) δ (ppm): 2.0754 (s), 2.3130 (s), 5.8387 (s), 5.9719 (s), 6.1056 (s), 7.5663 (s), 7.7373 (s), 7.9627 (s).

References

1. Natali, M.; Giordani, S. *Chem. Soc. Rev.* **2012**, *41*, 4010.
2. a) Qin, C.-G.; Lu, C.-X.; Ouyang, G.-W.; Qin, K.; Zhang, F.; Shi, H.-T.; Wang, X.-H. *Chinese J Anal Chem.* **2015**, *43*, 433. b) Liu, D.; Bastiaansen, C. W. M.; Den Toonder, J. M. J.; Broer, D. J. *Angew. Chem.* **2011**, *51*, 892.
3. a) Russew, M.-M.; Hecht, S. *Adv. Mater.* **2010**, *22*, 3348. b) Merino, E.; Ribagorda, M. Beilstein. *J Org Chem.* **2012**, *8*, 1071. c) Hüll, K.; Morstein, J.; Trauner, D. *Chem. Rev.* **2018**, *118*, 10710. d) Hoorens, M. W.; Szymanski, W. *Trends Biochem. Sci.* **2018**, *43*, 567. e) Gobbi, M.; Bonacchi, S.; Lian, J. X.; Vercouter, A.; Bertolazzi, S.; Zyska, B.; Timpel, M.; Tatti, R.; Olivier, Y.; Hecht, S.; Nardi, M. V.; Beljonne, D.; Orgiu, E.; Samorì, P. *Nat. Commun.* **2018**, *9,* 2661.
4. a) Harris, J. D.; Moran, M. J.; Aprahamian, I. *Proc. Natl. Acad. Sci. U. S. A.* **2018**, *115*, 9414. b) Pianowski, Z. L. *Chem.: Eur. J.* **2019**, *25*, 5128.
5. Bandara, H. M. D.; Burdette, S. C. *Chem. Soc. Rev*. **2012**, *41*, 1809.
6. Bléger, D.; Hecht, S. *Angew. Chem.* **2015**, *54*, 11338.
7. Calbo, J.; Weston, C. E.; White, A. J. P.; Rzepa, H. S.; Contreras-García, J.; Fuchter, M. J. *J. Am. Chem. Soc.* **2017**, *139*, 1261 .
8. a) Devi, S.; Saraswat, M.; Grewal, S.; Venkataramani, S. *J. Org. Chem.* **2018**, *83*, 4307.b) Simeth, N. A.; Bellisario, A.; Crespi, S.; Fagnoni, M.; König, B. *J. Phys. Chem. A.* **2019**, *123*, 1814.
9. Weston, C. E.; Richardson, R. D.; Haycock, P. R.; White, A. J. P.; Fuchter, M. J. *J. Am. Chem. Soc.* **2014**, *136*, 11878.
10. a) Stricker, L.; Fritz, E.-C.; Peterlechner, M.; Doltsinis, N. L.; Ravoo, B. J. *J. Am. Chem. Soc.* **2016**, *138*, 4547. b) Wiemann, M.; Niebuhr, R.; Juan, A.; Cavatorta, E.; Ravoo, B. J.; Jonkheijm, P. *Chem.: Eur. J* **2017**, *24*, 813. c) Adam, V.; Prusty, D. K.; Centola, M.; Škugor, M.; Hannam, J. S.; Valero, J.; Klöckner, B.; Famulok, M. *Chem.: Eur. J.* **2018**, *24*, 1062. d) Devi, S.; Gaur, A. K.; Gupta, D.; Saraswat, M.; Venkataramani, S. *ChemPhotoChem* **2018**, *2*, 806.
11. Ghebreyessus, K.; Cooper, S. M. *Organometallics* **2017**, *36*, 3360.

12. a) Ko, C.-C.; Yam, V. W.-W. *J. Mater. Chem*. **2010**, *20*, 2063. b) Tylkowski, B.; Trojanowska, A.; Marturano, V.; Nowak, M.; Marciniak, L.; Giamberini, M.; Ambrogi, V.; Cerruti, P. *Coord. Chem. Rev.* **2017**, *351*, 205.
13. a) Xue, X.; Wang, H.; Han, Y.; Hou, H. *Dalton Trans.* **2018**, *47*(1), 13–22. b) Ihrig, S. P.; Eisenreich, F.; Hecht, S. *Chem. Comm.* **2019**, *55*(30), 4290–4298. c) Chastanet, G.; Lorenc, M.; Bertoni, R.; Desplanches, C. *Comptes Rendus Acad. Sci.* **2018**, *21*, 1075.
14. Viciano-Chumillas, M.; Tanase, S.; Jongh, L. J. D.; Reedijk, J. *Eur. J. Inorg. Chem.* **2010**, *2010*, 3403.
15. Abd-El-Aziz, A. S.; Strohm, E. A. *Polym. J.* **2012**, *53*, 4879.
16. Massoud, S. S.; Louka, F. R.; David, R. N.; Dartez, M. J.; Nguyn, Q. L.; Labry, N. J.; Fischer, R. C.; Mautner, F. A. *Polyhedron* **2015**, *90*, 258.
17. Cubanski, J. R.; Reish, M. E.; Blackman, A. G.; Steel, P. J.; Gordon, K. C.; Mcmorran, D. A.; Crowley, J. D. *Aust. J. Chem.* **2015**, *68*, 1160.
18. Ajellal, N.; Kuhn, M. C. A.; Boff, A. D. G.; Hörner, M.; Thomas, C. M.; Carpentier, J.-F.; Casagrande, O. L. *Organometallics* **2006**, *25*, 1213.
19. Herchel, R.; Dvořák, Z.; Trávníček, Z.; Mikuriya, M.; Louka, F. R.; Mautner, F. A.; Massoud, S. S. *Inorganica Chim. Acta.* **2016**, *451*, 102.
20. Taddei, M.; Costantino, F.; Marmottini, F.; Comotti, A.; Sozzani, P.; Vivani, R. *Chem. Commun.* **2014**, *50*, 14831.

Appendix

NMR

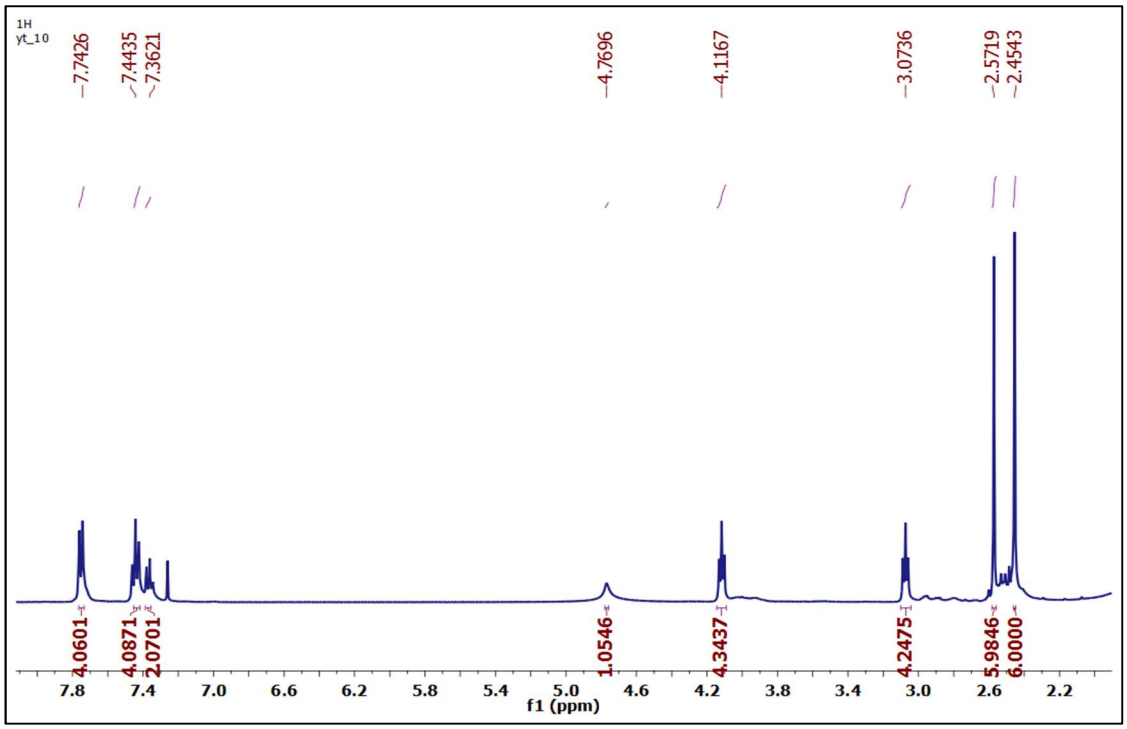

Fig A1. ^{1}H NMR spectrum of **L1.** (Solvent: $CDCl_3$; Concentration: 17.83 mM)

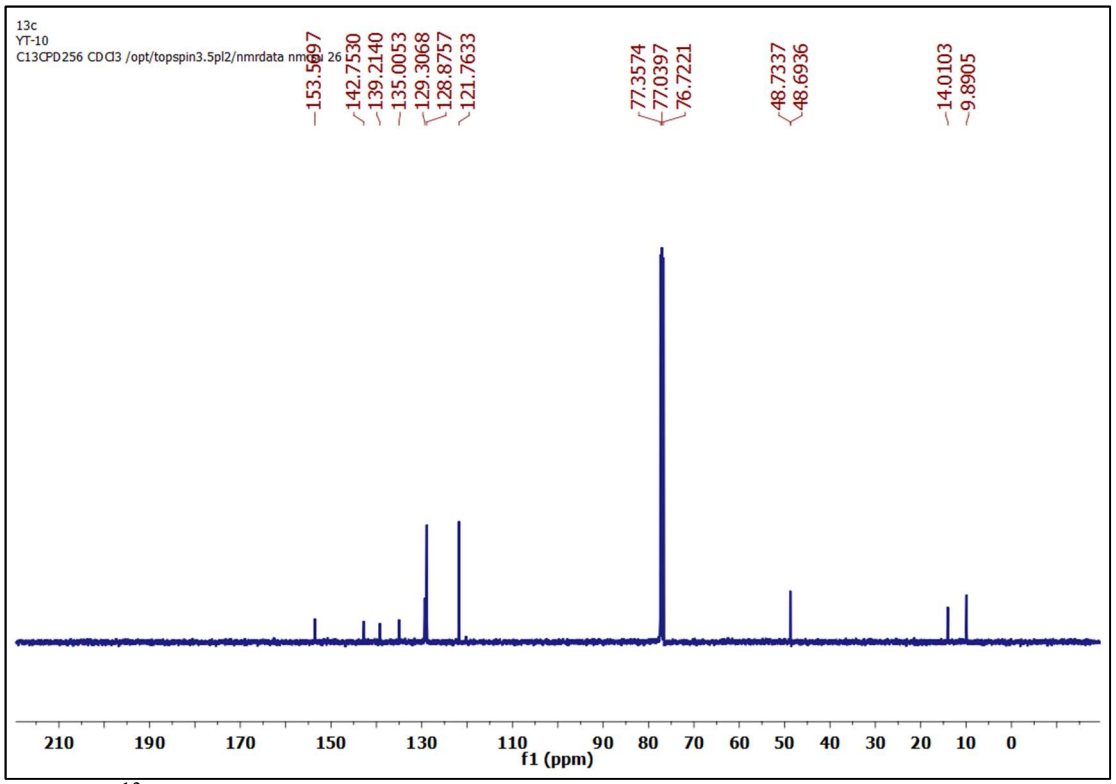

Fig A2. ^{13}C NMR spectrum of **L1.** (Solvent: $CDCl_3$; Concentration: 17.83 mM)

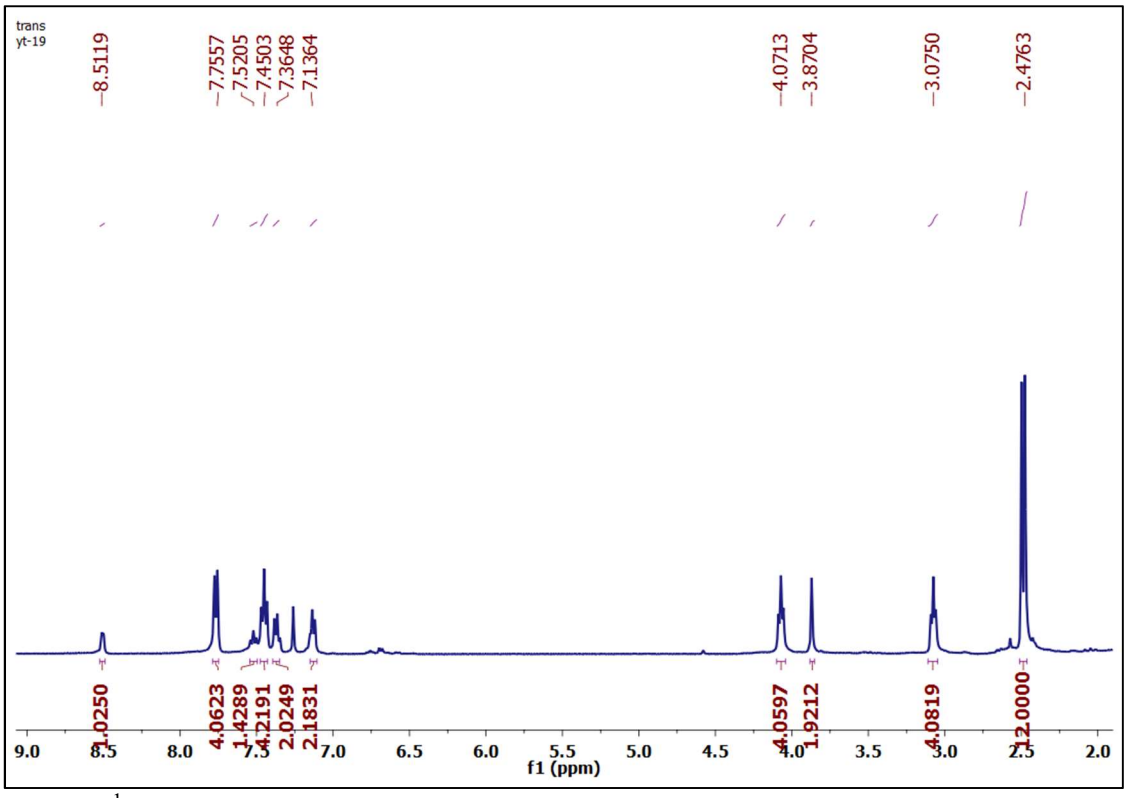

Fig A3. ^{1}H NMR spectrum of **L2.** (Solvent: $CDCl_3$; Concentration: 21.29 mM)

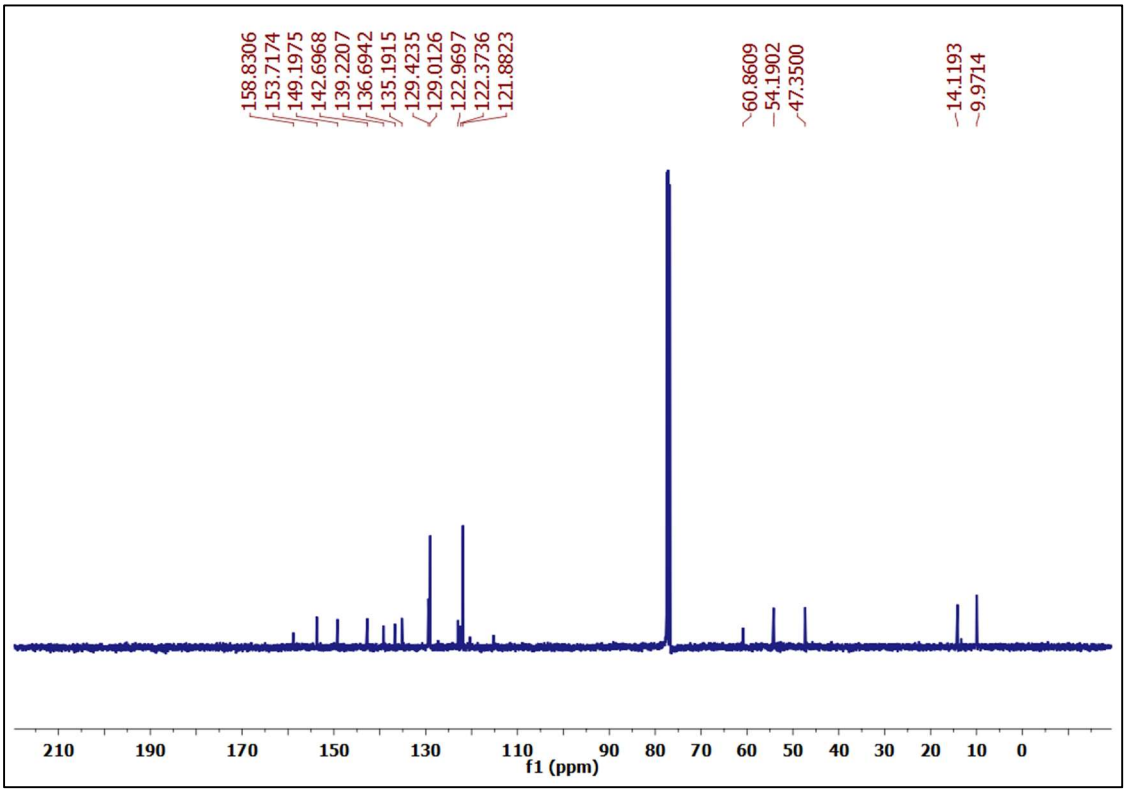

Fig A4. ^{13}C NMR spectrum of **L2.** (Solvent: $CDCl_3$; Concentration: 21.29 mM)

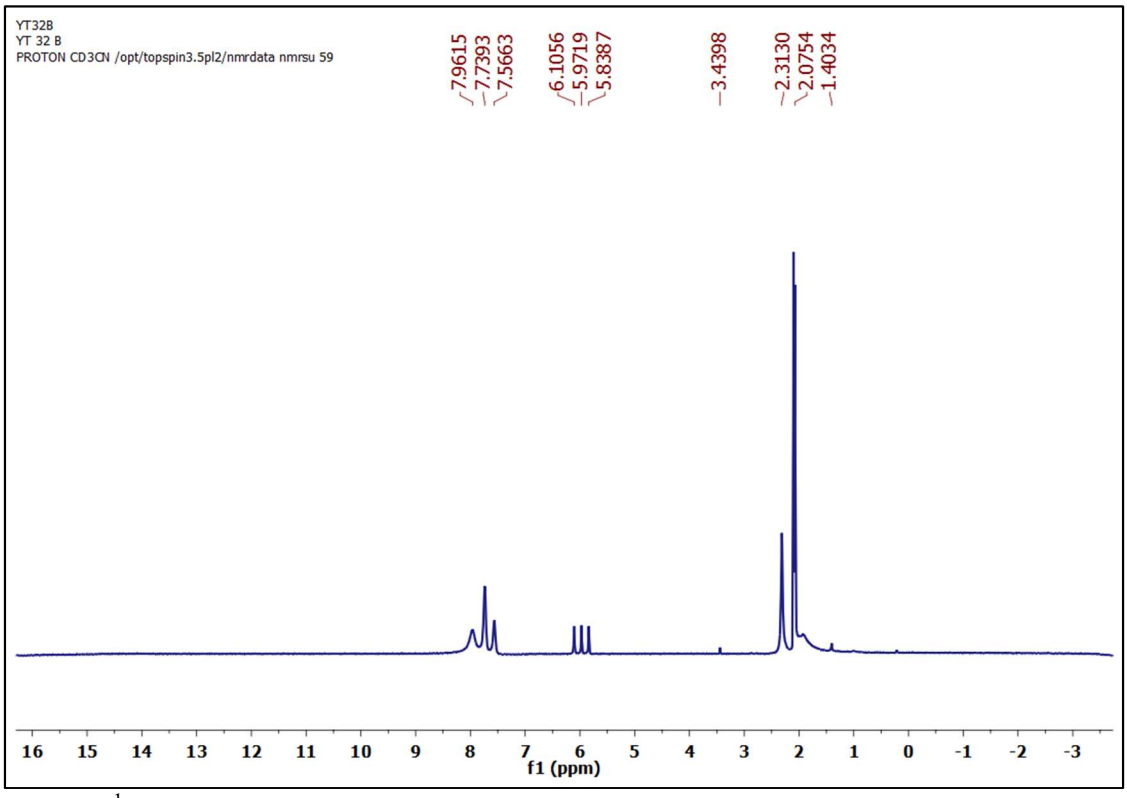

Fig A5. ^{1}H NMR spectrum of **1A**. (Solvent: CH_3CN; Concentration: 15.26 mM)

HRMS

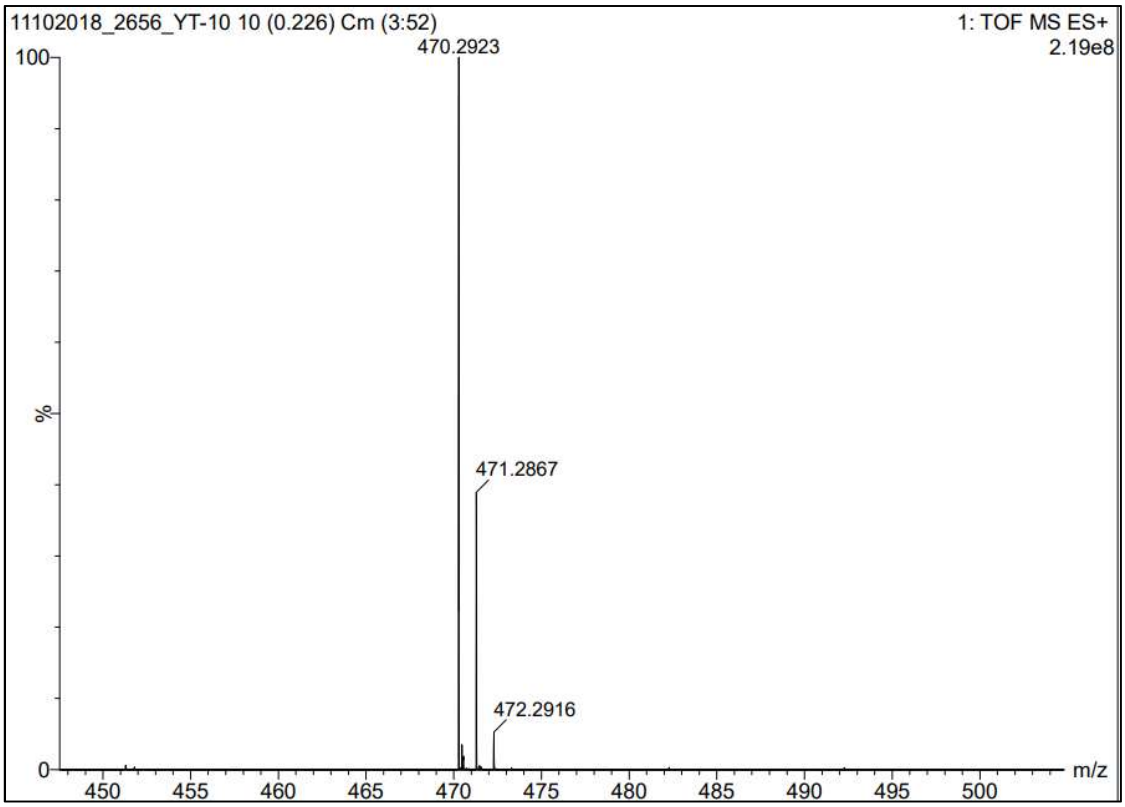

Fig A6. L1 HRMS

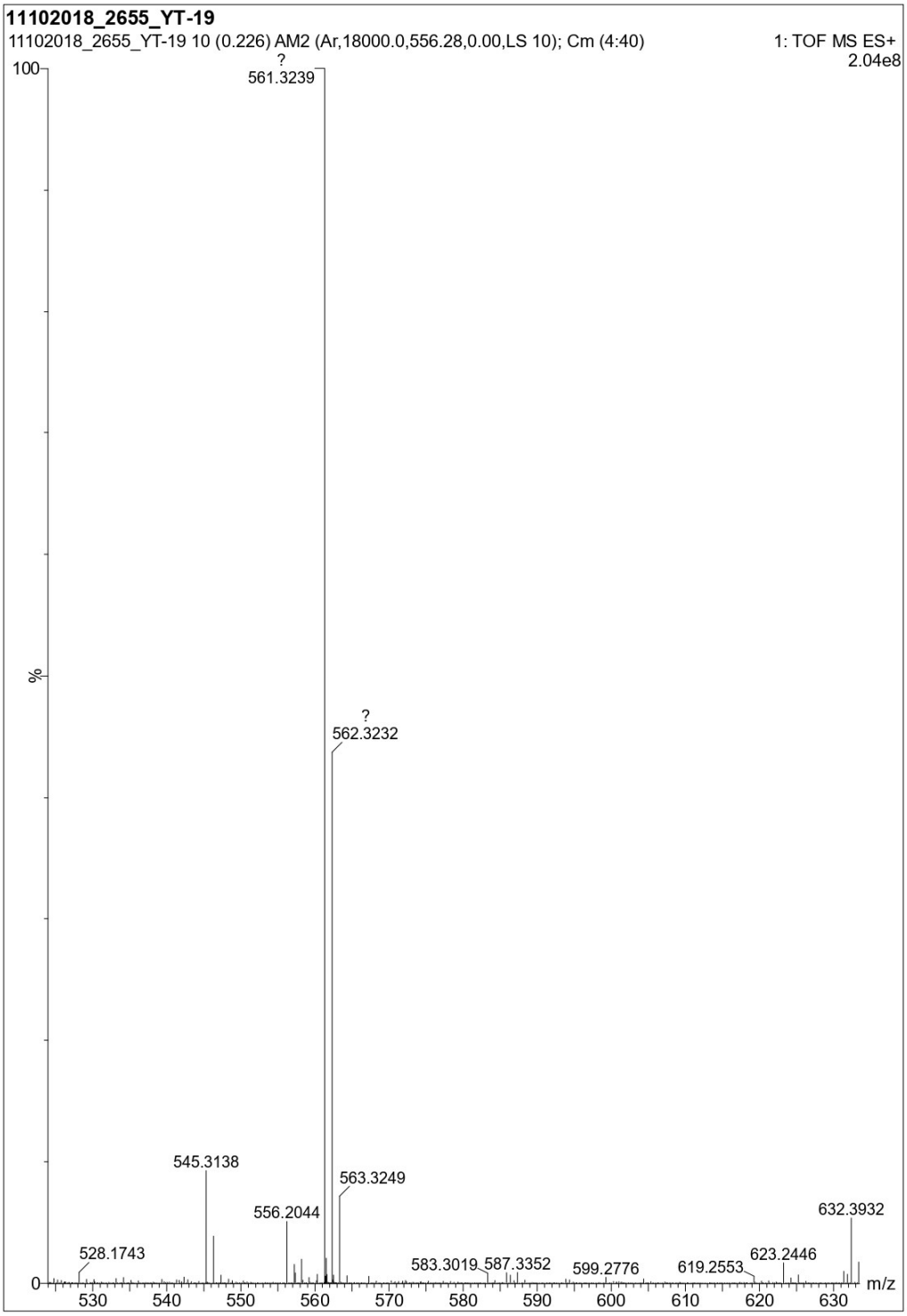

Fig A7. L2 HRMS

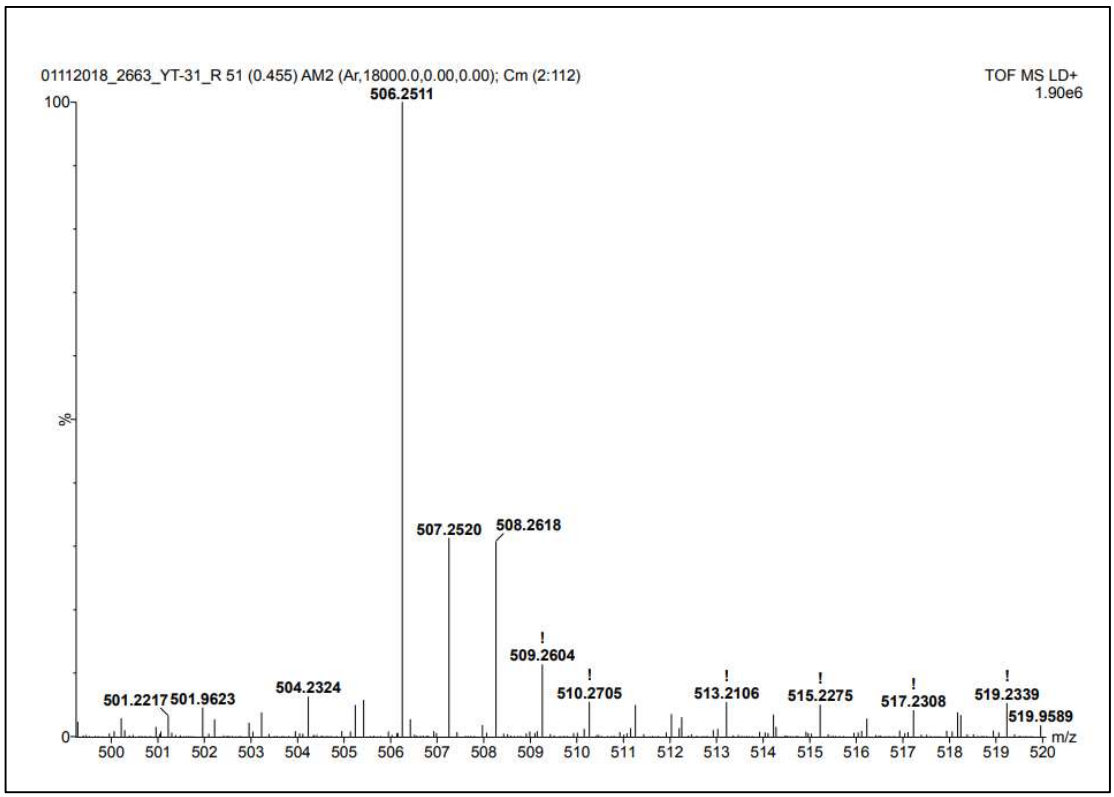

Fig A8. P2 HRMS

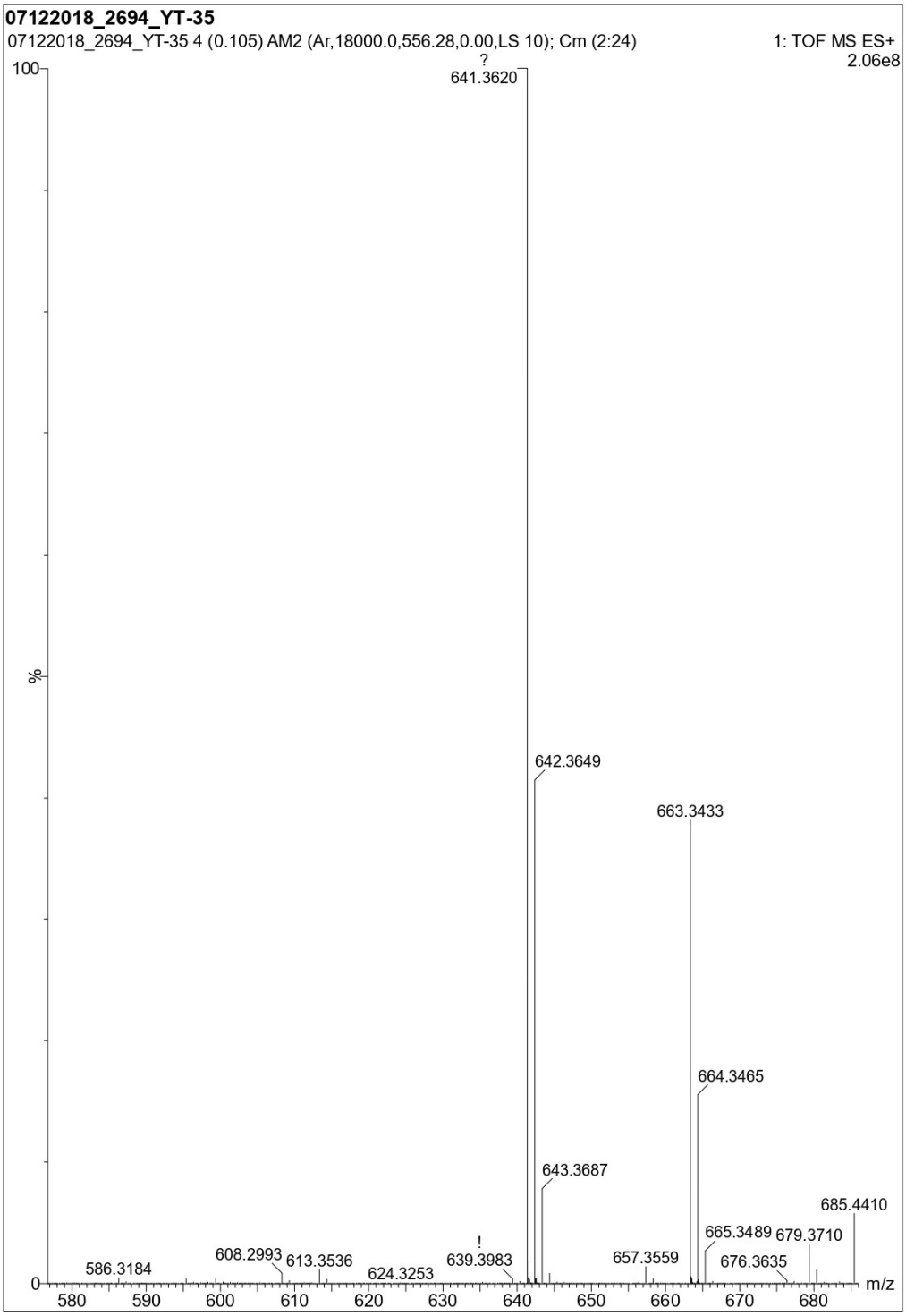

Fig A9. L3 HRMS

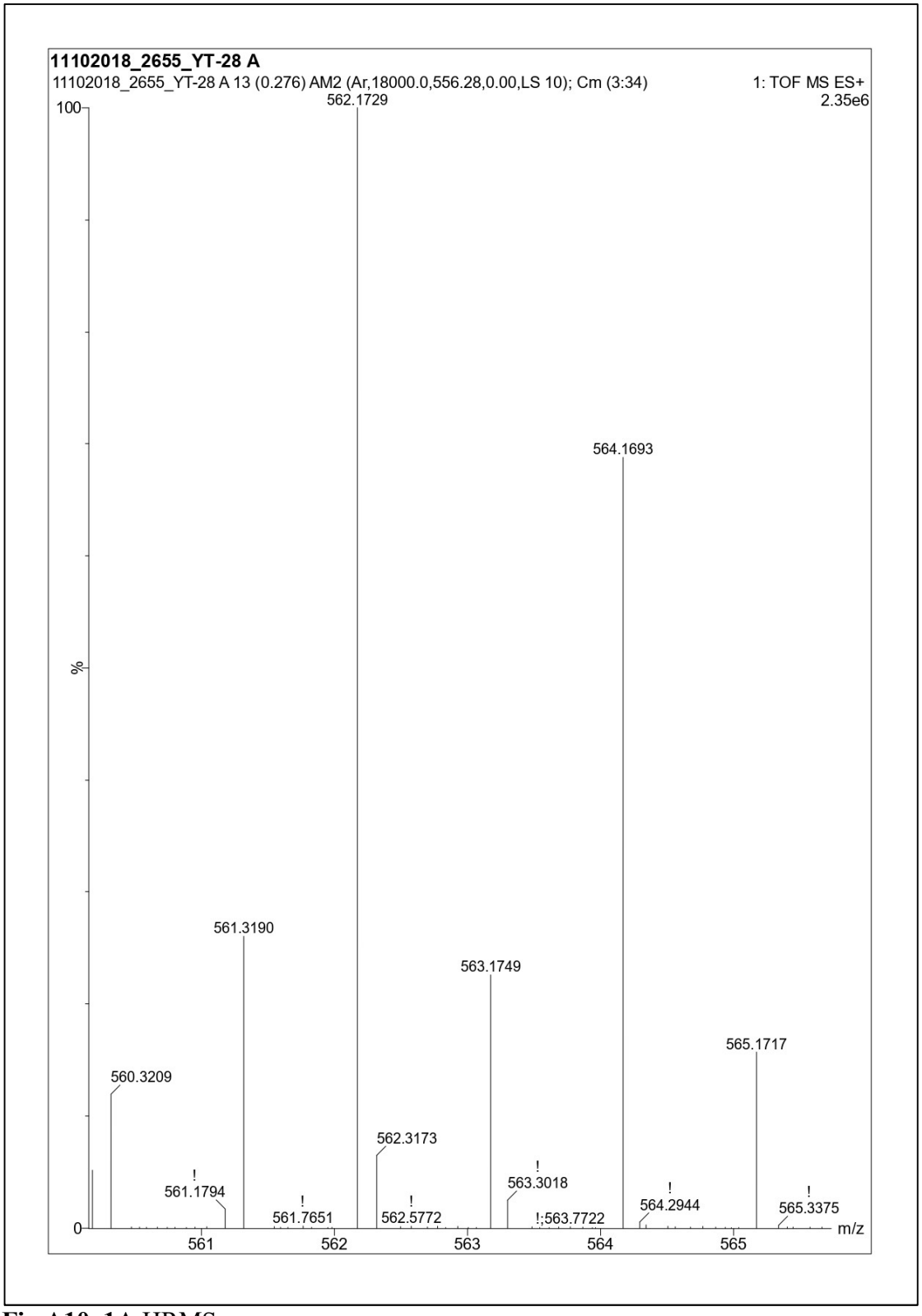

Fig A10. 1A HRMS

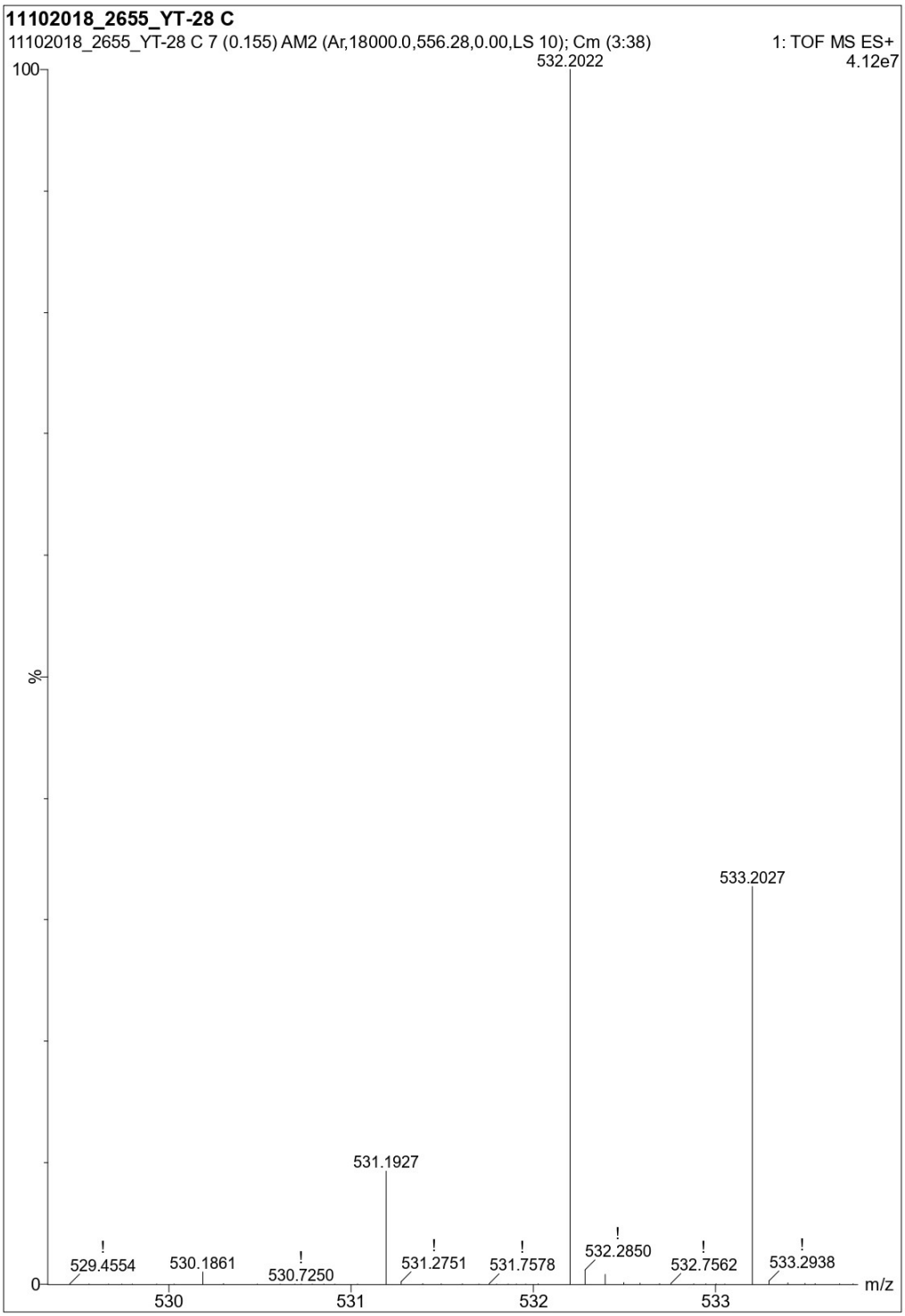

Fig A11. 1C HRMS

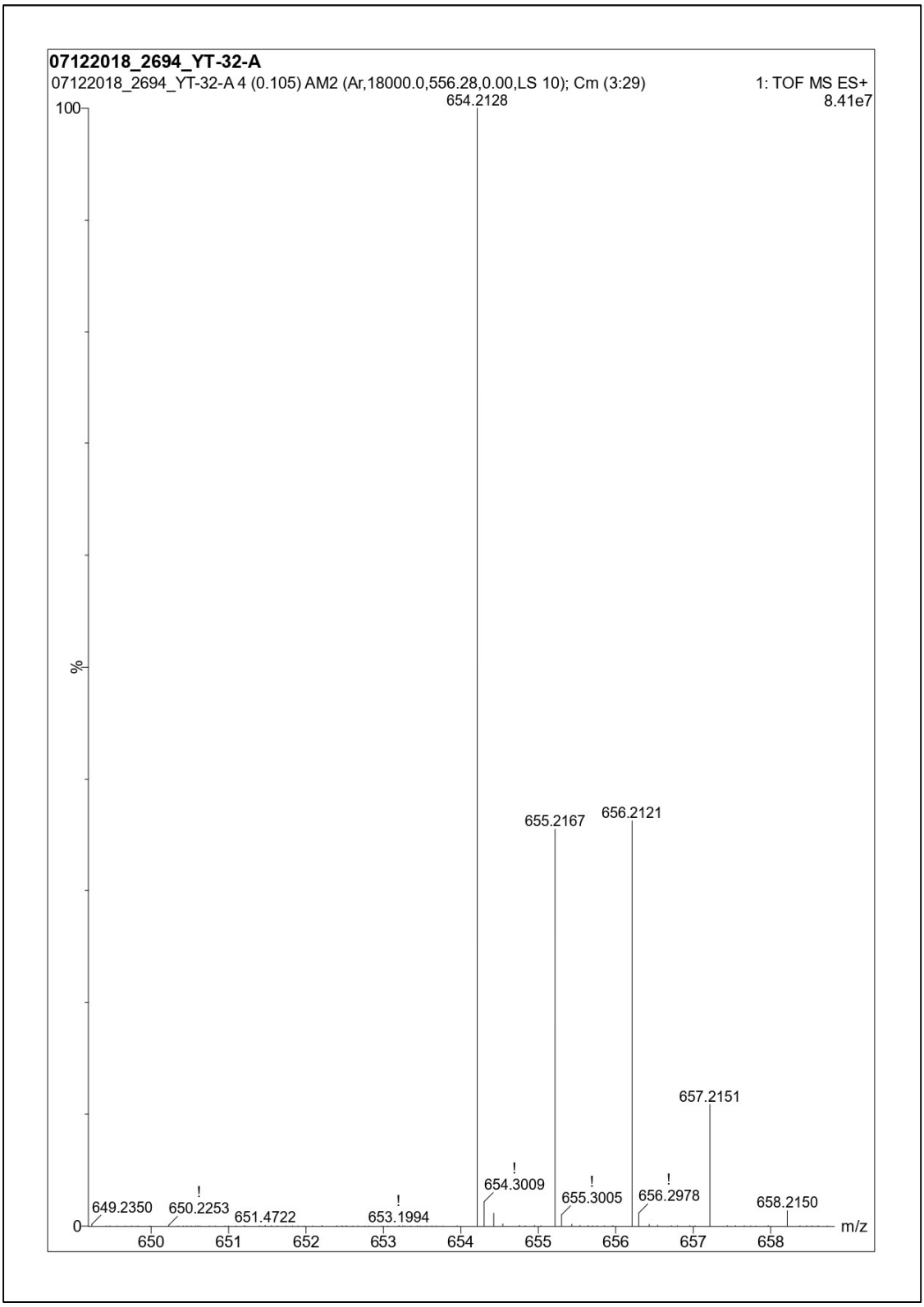

Fig A12. 2A HRMS

Compound[a]	**2B**
Chemical formula	C34 H39 Cl Cu F6 N11 P
Molar mass	845.72
Crystal system	Triclinic
Space group	*P* -1
T [K]	200.01(10)
a [Å]	9.83040(10)
b [Å]	12.06690(10)
c [Å]	16.5603(2)
α [°]	104.0100(10)
β [°]	96.3360(10)
γ [°]	101.1170(10)
V [Å3]	1844.60(3)
Z	2
D(calcd.) [g·cm–3]	1.523
μ(Mo-*K*α) [mm–1]	0.782
Index range	$-17 \leq h \leq 16$
	$-13 \leq k \leq 11$
	$-18 \leq l \leq 18$
Reflections collected	41198
Independent reflections	12842
Data/restraints/parameters	12842/0/492
*R*1,*wR*2[*I*>2*σ*(*I*)][a]	0.0400, 0.1044
R1, wR2 (all data)[a]	0.0508, 0.1156
GOF	1.081

[a] $R1 = \Sigma||Fo| - |Fc||/\Sigma|Fo|$. $wR2 = [\Sigma w(|Fo^2| - |Fc^2|)^2/\Sigma w|Fo^2|^2]^{1/2}$

Table A1. Single Crystal XRD data of **2B**

Vaitheesh Jeyapalan

Indian Institute of Science Education and Research, Mohali

ADDRESS

GG-9, GREEN GARDENS,
RAMANKULANGARA,
KAVANAD P.O, KOLLAM,
KERALA. 691003
ytheesh96@gmail.com
+91-7837704685

SKILLS

•Synthesis and characterization of organic molecules
•Separation techniques in Organic Chemistry lab :TLC, Column Chromatography
•Characterization Techniques: FTIR, UV-Vis, ATR, Fluorescence Spectroscopy, Differential Scanning Calorimetry
•Experience in spectral analysis such as NMR Spectrum, Mass Spectrum

COMPUTATIONAL SKILLS

Programming Languages: Python, C, Sage |
Tools: Gaussian09, Gauss view, Origin, Chemdraw, Origin, MestReNova

FELLOWSHIPS, CREDENTIALS

•DST INSPIRE fellowship at the undergraduate level from August 2014 to May 2019

RESEARCH EXPERIENCE

SUMMER INTERNSHIP • INDIAN INSTITUTE OF SPACE SCIENCE AND TECHNOLOGY, THIRUVANANTHAPURAM • 2015

Under the guidance of Dr. Gomathi N |Worked out a new procedure to synthesize graphene quantum dots | Winner : Poster presentation for the internships done at IIST during Summer 2015

SUMMER INTERNSHIP • IISERM • 2016

Under the guidance of Dr. P. Balanarayan | Computational study of molecular dynamics

SUMMER INTERNSHIP • IISERM • 2017

Under the guidance of Dr. Sugumar Venkataramani | Synthesis of different photo switchable azoheteroarenes

SUMMER INTERNSHIP • IISERM • 2018

Under the guidance of Dr. Sugumar Venkataramani |Synthesis of photo-controlled molecular systems capable of reversible encapsulation and release of guest molecules

FINAL YEAR THESIS • IISERM • 2018-2019

Under the guidance of Dr. Sugumar Venkataramani | Azoheteroarene Based Ligands for Metal Binding and Solid State Photochromism

EDUCATION

BS-MS DUAL DEGREE PROGRAM IN CHEMICAL SCIENCES • 2014- • INDIAN INSTITUTE OF SCIENCE EDUCATION AND RESEARCH MOHALI

Expected graduation date – May 2019 | Completed 9th Semester | SPI 9.6 | CPI 7.0

HIGHER SECONDARY EDUCATION • 2012 -2014 • ST. ANTONY'S PUBLIC SCHOOL ANAKKAL, KANJIRAPALLY, KOTTAYAM

Science subjects : Chemistry, Biology, Physics & Maths | Marks Aggregate 90%

SECONDARY EDUCATION • 2010-2012 • ST. MARY'S RESIDENTIAL CENTRAL SCHOOL, RAMANKULANGARA KOLLAM

Science Subjects : Chemistry, Biology, Physics, Computer Science & Maths | Marks Aggregate 95%

Vaitheesh Jeyapalan

Indian Institute of Science Education and Research, Mohali

•Participated in Frontiers in Chemical Sciences (2018), IIT Guwahati
•Among top 1 percentile in All India Higher Secondary Examinations conducted by the Central board of secondary education (CBSE)

LANGUAGES

Tamil-Native Proficiency
English-Full professional proficiency
Malayalam & Hindi-Bilingual Proficiency